Chemical Physics Reviews

REVIEW ARTICLE | FEBRUARY 12 2025

Light–matter interaction Hamiltonians in cavity quantum electrodynamics FREE

Michael A. D. Taylor ; Arkajit Mandal ; Pengfei Huo

Check for updates

Chem. Phys. Rev. 6, 011305 (2025)
https://doi.org/10.1063/5.0225932
CHORUS

View Online
Export Citation

Articles You May Be Interested In

Perturbative analysis of the coherent state transformation in *ab initio* cavity quantum electrodynamics

J. Chem. Phys. (November 2024)

Comparing parameterized and self-consistent approaches to *ab initio* cavity quantum electrodynamics for electronic strong coupling

J. Chem. Phys. (November 2024)

A quantum description of radiation damping and the free induction signal in magnetic resonance

J. Chem. Phys. (July 2013)

13 February 2025 02:07:04

AIP Publishing

Special Topics Open for Submissions

Learn More

AIP Publishing

Chemical Physics Reviews REVIEW pubs.aip.org/aip/cpr

Light–matter interaction Hamiltonians in cavity quantum electrodynamics

Cite as: Chem. Phys. Rev. 6, 011305 (2025); doi: 10.1063/5.0225932
Submitted: 27 June 2024 · Accepted: 13 January 2025 ·
Published Online: 12 February 2025

View Online Export Citation CrossMark

Michael A. D. Taylor,[1,a)] Arkajit Mandal,[2,a)] and Pengfei Huo[1,3,a)]

AFFILIATIONS

[1]Institute of Optics, Hajim School of Engineering, University of Rochester, Rochester, New York 14627, USA
[2]Department of Chemistry, Texas A&M University, College Station, Texas 77842, USA
[3]Department of Chemistry, University of Rochester, 120 Trustee Road, Rochester, New York 14627, USA

[a)]**Authors to whom correspondence should be addressed:** michael.taylor@rochester.edu; mandal@tamu.edu; and pengfei.huo@rochester.edu

ABSTRACT

When matter is strongly coupled to an optical cavity, new hybrid light–matter states are formed, the so-called polariton states. These polaritons can qualitatively change the physical properties of the matter coupled to the cavity by completely altering its energy eigenspectrum. Fueled by experimental innovations in recent years, much progress has been made in simulating the intrinsic quantum behavior of these hybrid states. At the heart of each simulation is the choice of Hamiltonian to represent the total light–matter hybrid system. Even at this fundamental level, there has been significant progress in developing new gauges and representations for this Hamiltonian, whether exact or under approximations. As such, this review aims to discuss several different forms of Hamiltonians for the researcher trying to enter this field by clearly and concisely deriving each different representation from the fundamental Minimal Coupling Hamiltonian. In addition, this review provides commentary on the optimal usage and extent of approximations for each individual representation to assist the reader in choosing the appropriate Hamiltonian for their work.

Published under an exclusive license by AIP Publishing. https://doi.org/10.1063/5.0225932

13 February 2025 02:07:04

TABLE OF CONTENTS

I. INTRODUCTION

Recent progress in enabling new chemical reactivities by strongly coupling molecular systems to quantized radiation[1–12] has stimulated theoretical developments in molecular quantum electrodynamics (see Fig. 1).[13–29] In particular, light–matter interactions beyond the weak–strong coupling regime, such as the ultra-strong coupling[28] (USC) and the deep-strong coupling[30] (DSC) regime, are currently an active field of theoretical research.[13,18,20,30–37] Such coupling regimes lead to new exciting physical phenomena that cannot be described with the widely used approximate light–matter Hamiltonians such as the Rabi and Jaynes–Cumming Hamiltonians[18,19,21,24,38] of quantum optics. In this manner, it is crucial to strategically choose which light–matter

Published under an exclusive license by AIP Publishing

Hamiltonian to use to model your system by understanding the different benefits and shortcomings of each representation.

As this field of cavity quantum electrodynamics (cQED) is highly interdisciplinary, drawing from both quantum optics and physical chemistry, the appropriate choice of Hamiltonian can be obfuscated for those new to the field. Often, the relationships between Hamiltonians and exact levels of approximation consequentially become unclear. In this review, we seek to put in one place all the major gauges and representations commonly used in the field with detailed derivations that relate them to each other, helping to bridge the gap between quantum optics and physical chemistry.

This review is organized such that exact Hamiltonians for matter coupled to a single mode are initially introduced in Sec. II, and Secs. III–V layer on approximations, going all the way to the semiclassical approximation. As such, Sec. II introduces different forms of the full Hilbert space Hamiltonian, derived from the fundamental Minimal Coupling Hamiltonian. Then, in Sec. III, the truncation of the full Hilbert space is considered, with discussions of the various methods for addressing the gauge ambiguities caused by such projections. In Sec. IV, the simplified quantum optics models are discussed and benchmarked relative to the truncated matter Hamiltonians. Then, Sec. V provides a brief comparison of cQED methods with Floquet theory, which is under the semiclassical approximation. Using insights from this path, Sec. VI extends the formalism to more generalized forms of cQED Hamiltonians for systems with many modes and many molecules. The future perspectives and analysis are provided in Sec. VII.

II. CAVITY QED HAMILTONIANS

Before directly discussing various exact cavity QED Hamiltonians, we define the formalism used in the rest of the review for the two primary degrees of freedom (DOF) covered in this review,

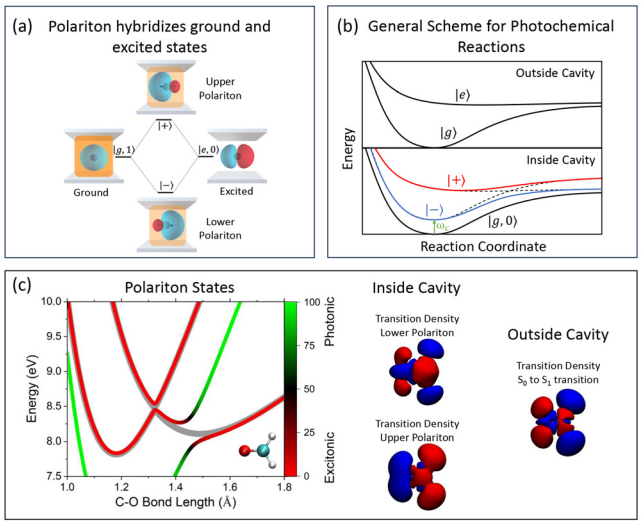

FIG. 1. Characteristic examples of polariton photochemistry. (a) Schematic illustration of Rabi splitting due to strong coupling for a single atom in a cavity. (b) Eigenspectra for a diatomic molecular system both outside and inside a cavity. (c) Properties of a formaldehyde molecule inside a cavity, demonstrating more complex polariton eigenspectra and changes in transition densities due to the cavity.[39] (Weight *et al.*, J. Phys. Chem. Lett. **14**, 5901–5913, 2023; licensed under a Creative Commons Attribution (CC BY 4.0) license.)

namely, the molecular Hamiltonian and the photonic Hamiltonian. Following this brief overview of these independent Hamiltonians, the rest of this section focuses on different representations of QED Hamiltonians that describe light–matter interactions: the minimal coupling Hamiltonian (Sec. II A), the dipole gauge Hamiltonian (Sec. II B), and the asymptotically decoupled Hamiltonian (Sec. II C).

We introduce the matter Hamiltonian in its most fundamental form as an ensemble of charged particles interacting with some potential. In our notation, we formulate this as

$$\hat{H}_{\mathrm{M}} = \hat{\mathbf{T}} + \hat{V}(\hat{\mathbf{x}}) = \sum_j \frac{1}{2m_j}\hat{\mathbf{p}}_j^2 + \hat{V}(\hat{\mathbf{x}}); \quad \hat{\boldsymbol{\mu}} = \sum_j z_j \hat{\mathbf{x}}_j, \tag{1}$$

where j is the index of the jth charged particle (including all electrons and nuclei), with the corresponding mass m_j and charge z_j. In addition, $\hat{\mathbf{x}} \equiv \{\hat{\mathbf{x}}_j\} = \{\hat{\mathbf{R}}, \hat{\mathbf{r}}\}$ with $\hat{\mathbf{R}}$ and $\hat{\mathbf{r}}$ representing the sets of nuclear and electronic coordinates, respectively, $\hat{\mathbf{p}} \equiv \{\hat{\mathbf{p}}_{\mathbf{R}}, \hat{\mathbf{p}}_{\mathbf{r}}\} \equiv \{\hat{\mathbf{p}}_j\}$ is the *mechanical* momentum operator as well as the canonical momentum operator, such that $\hat{\mathbf{p}}_j = -i\hbar\nabla_j$. Further, $\hat{\mathbf{T}} = \hat{\mathbf{T}}_{\mathbf{R}} + \hat{\mathbf{T}}_{\mathbf{r}}$ is the kinetic energy operator, where $\hat{\mathbf{T}}_{\mathbf{R}}$ and $\hat{\mathbf{T}}_{\mathbf{r}}$ represent the kinetic energy operator for nuclei and for electrons, respectively, and $\hat{V}(\hat{\mathbf{x}})$ is the potential operator that describes the Coulombic interactions among electrons and nuclei. Note that this fundamental form does not make any Born–Oppenheimer approximations and is in general, exact and impossible to solve for real systems. It is, however, perfectly well suited for toy model systems where an electron is interacting with some external potential, and this representation allows us to most clearly show the fundamental light–matter coupling as a starting point. For the purpose of this review, we do not focus on solving the matter system itself, instead highlighting how coupling to the cavity affects said matter system. For a more in-depth review of molecular Hamiltonians, see Appendix A.

For the majority of Hamiltonians discussed in this review, the matter system is assumed to already be solved, and the light–matter Hamiltonian is framed in the eigenbasis of the matter Hamiltonian. Additionally, the light–matter coupling terms are written as functions of other matter observables that are accessible from electronic structure methods and assumed to be expressed in the matter eigenbasis. Namely, these are the particles' momenta and the molecular dipole, which is more common for molecular systems.

As light is a many-mode ensemble of simple harmonic oscillators, the cavity Hamiltonian for a single mode is

$$\hat{H}_{\mathrm{ph}} = \hbar\omega_{\mathrm{c}}\left(\hat{a}^\dagger\hat{a} + \frac{1}{2}\right) = \frac{1}{2}(\hat{p}_{\mathrm{c}}^2 + \omega_{\mathrm{c}}^2\hat{q}_{\mathrm{c}}^2), \tag{2}$$

where ω_{c} is the frequency of the mode in the cavity, $\hat{a}^\dagger$ and $\hat{a}$ are the photonic creation and annihilation operators, and $\hat{q}_{\mathrm{c}} = \sqrt{\hbar/2\omega_{\mathrm{c}}}(\hat{a}^\dagger + \hat{a})$ and $\hat{p}_{\mathrm{c}} = i\sqrt{\hbar\omega_{\mathrm{c}}/2}(\hat{a}^\dagger - \hat{a})$ are the photonic coordinate and momentum operators, respectively. This is the simplest picture of a cavity's Hamiltonian. In principle, a given cavity can have many modes that couple to matter. Such situations are discussed in Secs. III E and VI; however, for the sake of clarity and concision, we introduce each major representation of the Hamiltonian with only one cavity mode with the understanding that all can be extended to many modes.

Aside from just the photonic Hamiltonian, another important cavity operator for gauge theory is the mode's vector potential. Choosing

13 February 2025 02:07:04

Published under an exclusive license by AIP Publishing

the Coulomb gauge, $\nabla \cdot \hat{\mathbf{A}} = 0$, the vector potential becomes purely transverse $\hat{\mathbf{A}} = \hat{\mathbf{A}}_\perp$. Under the long-wavelength approximation,

$$\hat{\mathbf{A}} = \mathbf{A}_0(\hat{a} + \hat{a}^\dagger) = \mathbf{A}_0\sqrt{2\omega_c/\hbar}\,\hat{q}_c, \tag{3}$$

where $\mathbf{A}_0 = \sqrt{\frac{\hbar}{2\omega_c\varepsilon_0\mathcal{V}}}\hat{\mathbf{e}}$ for a Fabry–Pérot cavity, with $\mathcal{V}$ as the quantization volume inside the cavity, ε_0 as the permittivity, and $\hat{\mathbf{e}}$ is the unit vector of the field polarization. This long-wavelength approximation explicitly assumes that the vector potential does not vary with its spatial coordinate. In practice, it is crucial to consider the length scales of the mode and the matter to be justified in making this approximation. For example, for a single small molecule system ($\sim$1 nm spatial extent) coupled to a cavity mode in the visible range ($2\pi c/\omega_c \sim 400$ nm), this level of approximation is valid. However, when considering extended matter systems such as 2D materials or a large ensemble of molecules, this level of approximation can break down.[40]

As with the single-mode approximation, we also make this long wavelength approximation throughout our derivations in Sec. II–V for clarity. Section VI acts as an example of how to relax both of these approximations. For a more in-depth review of quantum optics, see Appendix B.

A. The minimal coupling Hamiltonian

We begin our discussion of QED with the most fundamental light–matter Hamiltonian in QED, the minimal coupling Hamiltonian. This will act as the starting point for all derivations in this review. The minimal coupling QED Hamiltonian in the *Coulomb* gauge (the "p · A" form) is expressed as

$$\hat{H}_{\text{p·A}} = \sum_j \frac{1}{2m_j}(\hat{\mathbf{p}}_j - z_j\hat{\mathbf{A}})^2 + \hat{V}(\hat{\mathbf{x}}) + \hat{H}_{\text{ph}}, \tag{4}$$

where $\hat{\mathbf{p}}_j = -i\hbar\nabla_j$ is the *canonical* momentum operator for the jth particle.

This p · A Hamiltonian can be directly thought of as the photonic DOF performing a unitary boost on the matter DOF. We can formalize this boost as a unitary operator, the so-called Power–Zienau–Woolley (PZW) gauge transformation operator,[41,42] expressed as

$$\hat{U} = \exp\left[-\frac{i}{\hbar}\hat{\boldsymbol{\mu}}\cdot\hat{\mathbf{A}}\right] = \exp\left[-\frac{i}{\hbar}\hat{\boldsymbol{\mu}}\cdot\mathbf{A}_0(\hat{a}+\hat{a}^\dagger)\right], \tag{5}$$

or equivalently $\hat{U} = \exp[-\frac{i}{\hbar}\sqrt{2\omega_c/\hbar}\hat{\boldsymbol{\mu}}\mathbf{A}_0\hat{q}_c] = \exp[-\frac{i}{\hbar}(\sum_j z_j\hat{\mathbf{A}}\hat{\mathbf{x}}_j)]$.

Recall that a momentum boost operator $\hat{U}_p = e^{-\frac{i}{\hbar}p_0\hat{q}}$ displaces $\hat{p}$ by the amount of p_0, such that $\hat{U}_p\hat{O}(\hat{p})\hat{U}_p^\dagger = \hat{O}(\hat{p}+p_0)$. Hence, $\hat{U}$ is a boost operator for both the photonic momentum $\hat{p}_c$ by the amount of $\sqrt{2\omega_c/\hbar}\hat{\boldsymbol{\mu}}\mathbf{A_0}$, as well as for the matter momentum $\hat{\mathbf{p}}_j$ by the amount of $z_j\hat{\mathbf{A}}$. Using $\hat{U}^\dagger$ to boost the matter momentum, one can show that

$$\hat{H}_{\text{p·A}} = \hat{U}^\dagger\hat{H}_{\text{M}}\hat{U} + \hat{H}_{\text{ph}}, \tag{6}$$

hence $\hat{H}_{\text{p·A}}$ can be obtained[31] by a momentum boost with the amount of $-z_j\hat{\mathbf{A}}$ for $\hat{\mathbf{p}}_j$, then adding $\hat{H}_{\text{ph}}$. It should be noted that while we are using staying in the single-particle, single photonic mode picture for simplicity, the PZW operator in principle can be expressed for many particles and many modes beyond any long-wavelength approximation (see Sec. III F).[42–44]

B. The dipole gauge Hamiltonian

Now that we have introduced our starting point, we perform a unitary gauge transformation on the minimal coupling Hamiltonian to arrive at the more common dipole gauge Hamiltonian.[41,45] This QED Hamiltonian is similarly found using the PZW operator from Eq. (5) as

$$\begin{aligned}\hat{H}_{\text{d·E}} &= \hat{U}\hat{H}_{\text{p·A}}\hat{U}^\dagger = \hat{U}\hat{U}^\dagger\hat{H}_{\text{M}}\hat{U}\hat{U}^\dagger + \hat{U}\hat{H}_{\text{ph}}\hat{U}^\dagger \\ &= \hat{H}_{\text{M}} + \hbar\omega_c\left(\hat{a}^\dagger\hat{a} + \frac{1}{2}\right) + i\omega_c\hat{\boldsymbol{\mu}}\cdot\mathbf{A}_0(\hat{a}^\dagger - \hat{a}) + \frac{\omega_c}{\hbar}(\hat{\boldsymbol{\mu}}\cdot\mathbf{A}_0)^2,\end{aligned} \tag{7}$$

where we have used Eq. (6) to express $\hat{H}_{\text{p·A}}$, and the last three terms of the second line are the results of $\hat{U}\hat{H}_{\text{ph}}\hat{U}^\dagger$. Note that upon applying $\hat{U}^\dagger$ to $\hat{H}_{\text{p·A}}$, we are boosting the matter and photonic momenta such that $\hat{\mathbf{p}}_j \to \hat{\mathbf{p}}_j - z_j\hat{\mathbf{A}}$ and $\hat{p}_c \to \hat{p}_c - \sqrt{2\omega_c/\hbar}\hat{\boldsymbol{\mu}}\mathbf{A}_0$. This effectively pushes the interaction terms from matter the kinetic energy term to the photonic kinetic energy term. This can be explicitly seen by rewriting $\hat{H}_{\text{d·E}}$ in terms of $\hat{q}_c$ and $\hat{p}_c$,

$$\hat{H}_{\text{d·E}} = \hat{H}_{\text{M}} + \frac{1}{2}\omega_c^2\hat{q}_c^2 + \frac{1}{2}\left(\hat{p}_c + \sqrt{\frac{2\omega_c}{\hbar}}\hat{\boldsymbol{\mu}}\mathbf{A}_0\right)^2, \tag{8}$$

because the PZW operator boosts the photonic momentum $\hat{p}_c$ by $\sqrt{2\omega_c/\hbar}\hat{\boldsymbol{\mu}}\mathbf{A}_0$. Additionally, the term $\frac{\omega_c}{\hbar}(\hat{\boldsymbol{\mu}}\mathbf{A}_0)^2$ is commonly referred to as the dipole self-energy (DSE). Note that in the literature, Eqs. (7) and (8) are sometimes written in the multipolar gauge, where the transverse polarization field is used instead of the dipole operator.[43,46]

The widely used Pauli–Fierz (PF) QED Hamiltonian[17,21,39,47–54] in recent studies of polariton chemistry can be then obtained by using the following unitary transformation

$$\hat{U}_\phi = \exp\left[-i\frac{\pi}{2}\hat{a}^\dagger\hat{a}\right]. \tag{9}$$

Note that $\hat{U}_\phi\hat{a}^\dagger\hat{a}\hat{U}_\phi^\dagger = \hat{a}^\dagger\hat{a}$, $\hat{U}_\phi\hat{a}\hat{U}_\phi^\dagger = i\hat{a}$, and $\hat{U}_\phi\hat{a}^\dagger\hat{U}_\phi^\dagger = -i\hat{a}^\dagger$. By applying $\hat{U}_\phi$ on $\hat{H}_{\text{d·E}}$, we have the PF Hamiltonian as follows:

$$\begin{aligned}\hat{H}_{\text{PF}} &= \hat{U}_\phi\hat{H}_{\text{d·E}}\hat{U}_\phi^\dagger \\ &= \hat{H}_{\text{M}} + \hbar\omega_c\left(\hat{a}^\dagger\hat{a} + \frac{1}{2}\right) + \omega_c\hat{\boldsymbol{\mu}}\cdot\mathbf{A}_0(\hat{a}+\hat{a}^\dagger) + \frac{\omega_c}{\hbar}(\hat{\boldsymbol{\mu}}\cdot\mathbf{A}_0)^2 \\ &= \hat{H}_{\text{M}} + \frac{1}{2}\hat{p}_c^2 + \frac{1}{2}\omega_c^2\left(\hat{q}_c + \sqrt{\frac{2}{\hbar\omega_c}}\hat{\boldsymbol{\mu}}\cdot\mathbf{A_0}\right)^2.\end{aligned} \tag{10}$$

The above PF Hamiltonian has the advantage as a pure real Hamiltonian and the photonic DOF can be viewed[21,47] and computationally treated[55,56] as an additional "nuclear coordinate."

We emphasize that both the **operators** and the **wavefunctions** should be gauge transformed (though $\hat{U}$), in order to have a gauge invariant expectation values. This means that

$$\hat{O} \to \hat{U}\hat{O}\hat{U}^\dagger, \quad |\Psi\rangle \to \hat{U}|\Psi\rangle, \tag{11}$$

13 February 2025 02:07:04

Published under an exclusive license by AIP Publishing

such that $\langle\hat{O}\rangle = \langle\Psi|\hat{O}|\Psi\rangle = (\langle\Psi|\hat{U}^\dagger)(\hat{U}\hat{O}\hat{U}^\dagger)(\hat{U}|\Psi\rangle)$. In the case of global unitary transforms (no spatial or momentum dependence), this is equivalent to simply writing the matrix/vector expressions of the operator/wavefunction in the new basis. Even though gauge transformations are not as simple as a basis change, the same principle applies.

For cavity QED, this principle is particularly salient for the photon number operator, as it is commonly asked, "how many photons are in the cavity?"[18,20] In response to this, the Coulomb gauge result is taken to be the physical photon number[18] and is defined as

$$\hat{N}_{\text{p-A}} = \hat{a}^\dagger\hat{a} = \frac{1}{2\hbar\omega_c}\hat{p}_c^2 + \frac{\omega_c}{2\hbar}\hat{q}_c^2 - \frac{1}{2}. \tag{12}$$

Under the dipole gauge, it should be

$$\begin{aligned}\hat{N}_{\text{d-E}} &= \hat{U}\hat{a}^\dagger\hat{a}\hat{U}^\dagger = \hat{U}\hat{a}^\dagger\hat{U}^\dagger\hat{U}\hat{a}\hat{U}^\dagger \equiv \hat{d}^\dagger\hat{d},\\ &= \frac{1}{2\hbar\omega_c}\left(\hat{p}_c + \sqrt{\frac{2\omega_c}{\hbar}}\hat{\boldsymbol{\mu}}\mathbf{A}_0\right)^2 + \frac{\omega_c}{2\hbar}\hat{q}_{\text{p-A}}^2 - \frac{1}{2},\end{aligned} \tag{13}$$

where $\hat{d}^\dagger = \hat{U}\hat{a}^\dagger\hat{U}^\dagger = \sqrt{\frac{\omega_c}{2\hbar}}\hat{U}\left(\hat{q}_c - \frac{i}{\omega}\hat{p}_c\right)\hat{U}^\dagger = \sqrt{\frac{\omega_c}{2\hbar}}[\hat{q}_c - \frac{i}{\omega}(\hat{p}_c + \sqrt{2\omega_c/\hbar}\hat{\boldsymbol{\mu}}\mathbf{A}_0)]$. For the PF Hamiltonian, the photon number operator should then be

$$\begin{aligned}\hat{N}_{\text{PF}} &= \hat{U}_\phi\hat{U}\hat{a}^\dagger\hat{a}\hat{U}^\dagger\hat{U}_\phi^\dagger = (\hat{U}_\phi\hat{U}\hat{a}^\dagger\hat{U}^\dagger\hat{U}_\phi^\dagger)(\hat{U}_\phi\hat{U}\hat{a}\hat{U}^\dagger\hat{U}_\phi^\dagger) \equiv \hat{c}^\dagger\hat{c}\\ &= \frac{1}{2\hbar\omega_c}\hat{p}_c^2 + \frac{\omega_c}{2\hbar}\left(\hat{q}_c + \sqrt{\frac{2}{\hbar\omega_c}}\hat{\boldsymbol{\mu}}\cdot\mathbf{A}_0\right)^2 - \frac{1}{2},\end{aligned} \tag{14}$$

where

$$\hat{c}^\dagger = \hat{U}_\phi\hat{U}\hat{a}^\dagger\hat{U}^\dagger\hat{U}_\phi^\dagger = \sqrt{\frac{\omega_c}{2\hbar}}\left[\left(\hat{q}_c + \sqrt{\frac{2\omega_c}{\hbar}}\hat{\boldsymbol{\mu}}\mathbf{A}_0\right) - \frac{i}{\omega_c}\hat{p}_c\right], \tag{15}$$

and the physical number operator is

$$\hat{N} = \hat{U}_\phi\hat{U}\hat{a}^\dagger\hat{a}\hat{U}^\dagger\hat{U}_\phi^\dagger = \hat{c}^\dagger\hat{c} \neq \hat{a}^\dagger\hat{a}. \tag{16}$$

This has been pointed out extensively in Refs. 18 and 20. Using the incorrect expression $\hat{a}^\dagger\hat{a}$ under the dipole gauge will overestimate the actual photon number, causing inaccurate and misleading results.

C. Asymptotically decoupled Hamiltonian

While the Coulomb and dipole gauges are by far the most common representations for light–matter couplings, in recent works, the asymptotically decoupled AD Hamiltonian was introduced to increase the simulation accuracy for models with arbitrarily strong coupling strengths.[35,40] We begin by rewriting $\hat{H}_{\text{p-A}}$ from Eq. (4) in its expanded form

$$\hat{H}_{\text{p-A}} = \hat{H}_{\text{M}} + \hbar\omega_c\hat{a}^\dagger\hat{a} + \frac{\hat{\mathbf{p}}\cdot\mathbf{A}_0}{m}(\hat{a}^\dagger + \hat{a}) + \frac{|\mathbf{A}_0|^2}{2m}(\hat{a}^\dagger + \hat{a})^2, \tag{17}$$

where the zero point energy of the photonic mode is omitted for simplicity. Then we perform a Bogoliubov transformation on the photonic degrees of freedom to rewrite $\hat{H}_{\text{p-A}}$ as

$$\hat{H}_{\text{p-A}} = \hat{H}_{\text{M}} + \hbar\Omega\hat{b}^\dagger\hat{b} - x_\Omega\mathbf{g}\cdot\hat{\mathbf{p}}(\hat{b}^\dagger + \hat{b}), \tag{18}$$

where $\Omega = \sqrt{\omega_c^2 + 2N|\mathbf{g}|^2}$ is the dressed photon frequency with a particle number N, $\mathbf{g} = q\mathbf{A_0}\sqrt{\omega_c/m\hbar}$ is the coupling strength, and $x_\Omega = \sqrt{\hbar/m\Omega}$ is a characteristic length. The Bogoliubov transform used in Eq. (18) is of the form, $\hat{b} + \hat{b}^\dagger = \sqrt{\Omega/\omega_c}(\hat{a} + \hat{a}^\dagger)$ to remove the linear term in $(\hat{a} + \hat{a}^\dagger)$ from Eq. (17).

Recall that a position shift operator, $\hat{U}_q = e^{-\frac{i}{\hbar}q_0\hat{p}}$ displaces $\hat{q}$ by the amount q_0, such that $\hat{U}_q\hat{O}(\hat{q})\hat{U}_q^\dagger = \hat{O}(\hat{q} + q_0)$. With this in mind, a shift operator in both photonic and matter coordinates is introduced, which transforms Eq. (18) into the AD representation

$$\hat{U}_{\text{AD}} = \exp\left[-\frac{i}{\hbar}\boldsymbol{\xi}_\mathbf{g}\cdot\hat{\mathbf{p}}\hat{\pi}\right], \tag{19}$$

where $\hat{\pi} = i(\hat{b}^\dagger - \hat{b})$ is the photonic momentum in the Bogoliubov transformed space and $\boldsymbol{\xi}_\mathbf{g} = \mathbf{g}x_\Omega/\Omega$ is an effective coupling parameter in the AD representation. This leads to the introduction of the AD Hamiltonian, $\hat{H}_{\text{AD}} = \hat{U}_{\text{AD}}^\dagger\hat{H}_{\text{p-A}}\hat{U}_{\text{AD}}$,

$$\hat{H}_{\text{AD}} = \sum_j\frac{1}{2m_j}\hat{\mathbf{p}}_j^2 + \hat{V}(\hat{\mathbf{x}}_j + \boldsymbol{\xi}_\mathbf{g}\hat{\pi}) + \hbar\Omega\hat{b}^\dagger\hat{b} - \sum_j\frac{\hbar^2g^2}{m_j\Omega^2}\hat{\mathbf{p}}_j^2. \tag{20}$$

By rescaling the mass of each particle to an effective mass, $m_j^{\text{eff}} = m_j[1 + 2|\mathbf{g}/\omega_c|^2]$, this asymptotically decoupled Hamiltonian is then simplified to

$$\hat{H}_{\text{AD}} = \sum_j\frac{1}{2m_j^{\text{eff}}}\hat{\mathbf{p}}_j^2 + \hat{V}(\hat{\mathbf{x}}_j + \boldsymbol{\xi}_\mathbf{g}\hat{\pi}) + \hbar\Omega\hat{b}^\dagger\hat{b}. \tag{21}$$

This is simply a photonic Hamiltonian added to a matter Hamiltonian with an effective mass scaling in the kinetic energy and a shift in coordinates in the potential energy. Note that the coupling is mediated by the shifting of each $\mathbf{x_j}$ by the photonic operator weighted by an effective coupling term $\boldsymbol{\xi}_\mathbf{g}$. However, $|\boldsymbol{\xi}_\mathbf{g}(\mathbf{g})|$ has a finite peak and then asymptotically approaches zero for large $|\mathbf{g}|$. In other words, in this representation, the photonic and matter degrees of freedom asymptotically decouple at arbitrarily high coupling strength. For this reason, this representation was put forward as a convenient Hamiltonian when considering systems in the deep strong coupling regime and beyond.

This AD Hamiltonian has also been expanded upon in recent work for solid-state materials in reciprocal space in Ref. 40, but is beyond the scope of this review as we are focused on molecular QED (Fig. 1).

III. QED HAMILTONIANS IN TRUNCATED HILBERT SPACES

Investigating the cavity QED computationally always requires a truncation of electronic states applied to the QED Hamiltonians,[31,33] as the electronic Hilbert space in principle has an infinite basis size for any real system. Additionally, as these matter electronic states are often difficult to obtain, one typically projects the QED Hamiltonian to a few physically relevant electronic states, which can still produce accurate results in the low energy regime. However, when dealing with strong light–matter coupling, the manner in which the truncation of the Hilbert space is performed drastically changes the accuracy and consequentially the convergence of results with basis size. In the context of this review, we assume that simulations are done via direct diagonalization of the Hamiltonian (instead of perturbative or similarly

13 February 2025 02:07:04

Published under an exclusive license by AIP Publishing

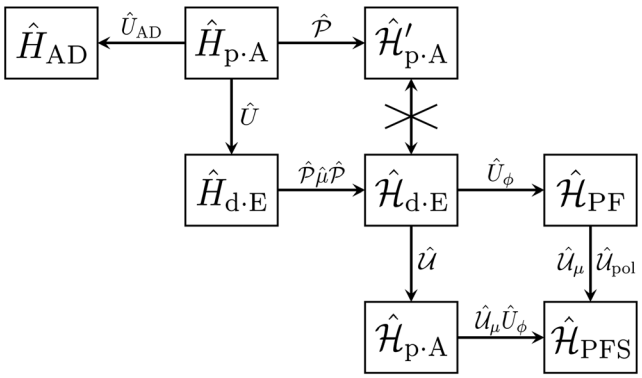

FIG. 2. Block diagram describing the relationships between various Hamiltonians discussed in this article. Hamiltonians in the top row have poor matter state convergence properties. Hamiltonians in the second row have poor Fock state convergence properties. Hamiltonians in the bottom row have good matter and Fock state convergence properties.

approximate approaches), benchmarking the different Hamiltonians by the minimum basis size required for their eigenenergies to converge.

Additionally, as with any truncation, the choice of basis is fundamental in determining the validity of said truncation. While for the photonic DOF, we always choose to truncate in the Fock basis, for matter DOFs there are a few commonly chosen bases that are discussed in this review. Foremost among these is the adiabatic basis. These are the eigensolutions to the electronic Hamiltonian (the matter Hamiltonian excluding the nuclear kinetic energy). While these are convenient states to obtain via electronic structure, they are in principle parameterized by the nuclear DOFs. In contrast to these are the diabatic states, which are independent of the nuclear coordinate. However, these diabatic states are difficult to obtain with exact solutions not existing beyond simple systems. As such, the Mulliken–Hush quasi-diabats can be used as approximate diabatic states for small changes in the nuclear configuration. In this section, all three of these basis choices are used to demonstrate the behavior of truncating the light–matter Hamiltonians, but the fundamental idea of gauge ambiguities and how to properly truncate the matter DOF is independent of the matter basis choice.

As such, this section reviews the recent literature results on truncating the Hilbert space of these QED systems. Sections III B and III C discuss two different ways to truncate the matter DOF of the dipole and Coulomb gauge Hamiltonians from Secs. II A and II B. Then, Sec. III D discusses a new representation of the light–matter coupling in a truncated Hilbert space, the polarized Fock state (PFS) Hamiltonian. Finally, Secs. III E and III F briefly discuss how performing truncations applies for more general systems with many modes and beyond the long-wavelength approximation, respectively (Note that the full descriptions for these generalized systems are found in Sec. VI.)

A. Benchmark model computational details

To accurately illustrate the performance of different truncated QED Hamiltonians, we test the accuracy of the Hamiltonians discussed in this review on a model molecular system inside a cavity of frequency $\omega_c = 400\,\mathrm{meV}$. Figure 3 shows the potential energy

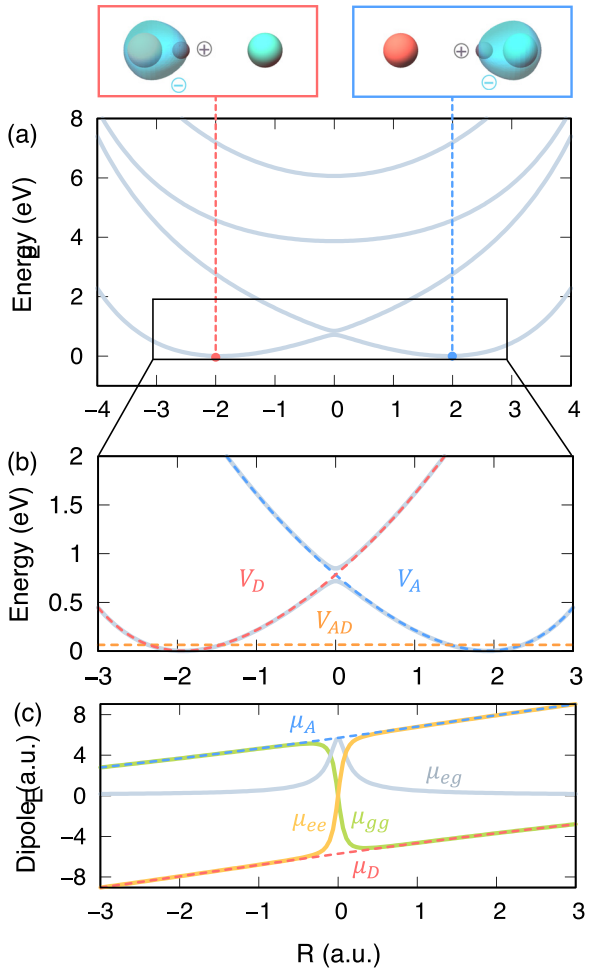

FIG. 3. Shin-Metiu model molecular system using parameters listed in Table I. (a) Potential energy surfaces of the first four molecular states. (b) Diabatic potentials (dashed curves) $V_{\mathrm{d\cdot E}}(R)$ (red) and $V_{\mathrm{A}}(R)$ (blue), with diabatic coupling V_{AD} (gold). (c) Matrix elements of $\hat{\mu}$ in the adiabatic representation (solid) μ_{gg} (green), μ_{ee} (orange), and μ_{eg} (light blue), as well as in the diabatic representation (dashed curves) $\mu_{\mathrm{d\cdot E}}$ (red) and μ_{A} (blue).

surfaces, diabatic potentials, and dipole matrix elements of the model system that we use to benchmark these Hamiltonians, the so-called Shin–Metiu proton-transfer model system.

This Shin–Metiu model molecular system[57] contains two fixed ions, one moving electron, and a proton (whose position is R), all interacting with each other through modified Coulombic potentials. These model potentials are characterized by a total Hamiltonian of $\hat{H}_{\mathrm{M}} = \hat{T}_R + \hat{H}_{\mathrm{el}}$, where $\hat{T}_R = \hat{P}_R^2/2m_{\mathrm{p}}$ is the kinetic energy of the transferring proton, with the proton mass m_{p}. $\hat{H}_{\mathrm{el}}$ is the electronic Hamiltonian

$$\hat{H}_{\mathrm{el}} = \hat{T}_r + \hat{V}_{\mathrm{eN}} + \hat{V}_{\mathrm{NN}}, \tag{22}$$

where $\hat{T}_r = \hat{p}_{\mathrm{r}}^2/2m_{\mathrm{e}}$ represents the kinetic energy operator of the single electron with mass m_{e}. As this is a single-dimensional model

13 February 2025 02:07:04

Published under an exclusive license by AIP Publishing

system, the electron-nuclei potential term, $\hat{V}_{\mathrm{eN}}$ is a modified Coulomb potential expressed as

$$\hat{V}_{\mathrm{eN}} = -z_{\mathrm{p}}e^2\frac{\mathrm{erf}\left(\frac{|r-R|}{R_{\mathrm{c}}}\right)}{|r-R|} - z_{\mathrm{D}}e^2\frac{\mathrm{erf}\left(\frac{|r-R_{\mathrm{D}}|}{R_{\mathrm{c}}}\right)}{|r-R_{\mathrm{D}}|} - z_{\mathrm{A}}e^2\frac{\mathrm{erf}\left(\frac{|r-R_{\mathrm{A}}|}{R_{\mathrm{c}}}\right)}{|r-R_{\mathrm{A}}|}, \tag{23}$$

where r is the electronic coordinate and $e = 1$ a.u. is the fundamental charge, R is the proton coordinate, while R_{D} and R_{A} are the positions of the static donor and acceptor ions, respectively. Furthermore, z_{p}, z_{D}, and z_{A} represent the charge of the proton, donor ion, and acceptor ion, respectively. Additionally, R_{c} characterizes the degree of shielding of the modified Coulomb interaction between the electron and the ions, where under the limit of $R_{\mathrm{c}} \to 0$, we recover the unshielded Coulomb potential.

The nuclear–nuclear interaction potential V_{NN} is similarly a modified Coulomb potential between the proton and the ions, expressed as

$$V_{\mathrm{NN}} = z_{\mathrm{p}}z_{\mathrm{D}}e^2\frac{\mathrm{erf}\left(\frac{|R-R_{\mathrm{D}}|}{R_{\mathrm{n}}}\right)}{|R-R_{\mathrm{D}}|} + z_{\mathrm{p}}z_{\mathrm{A}}e^2\frac{\mathrm{erf}\left(\frac{|R-R_{\mathrm{A}}|}{R_{\mathrm{n}}}\right)}{|R-R_{\mathrm{A}}|}, \tag{24}$$

where R_{n} is the nuclear–nuclear analog to R_{c}. The parameter values of the Shin–Metiu model used in this review are tabulated in Table I. All numerical results in this review assume this model system for the matter Hamiltonian.

B. Dipole and Coulomb gauge Hamiltonians

We begin with the simplest case of matter truncation. Consider a finite subset of electronic states $\{|\alpha\rangle\}$, where the projection operator $\hat{\mathcal{P}} = \sum_\alpha |\alpha\rangle\langle\alpha|$ defines the truncation of the full electronic Hilbert space $\hat{\mathbb{1}}_{\mathrm{r}} = \hat{\mathcal{P}} + \hat{\mathcal{Q}}$ to the corresponding subspace $\hat{\mathcal{P}}$. This truncation reduces the size of the Hilbert space from originally $\hat{\mathbb{1}}_{\mathrm{r}} \otimes \hat{\mathbb{1}}_{\mathrm{R}} \otimes \hat{\mathbb{1}}_{\mathrm{ph}}$ to now $\hat{\mathcal{P}} \otimes \hat{\mathbb{1}}_{\mathrm{R}} \otimes \hat{\mathbb{1}}_{\mathrm{ph}}$, where $\hat{\mathbb{1}}_{\mathrm{R}}$ and $\hat{\mathbb{1}}_{\mathrm{ph}}$ represent the identity operators of the nuclear and photonic DOF, respectively. The truncated matter Hamiltonian is

$$\hat{\mathcal{H}}_{\mathrm{M}} = \hat{\mathcal{P}}\hat{H}_{\mathrm{M}}\hat{\mathcal{P}} = \hat{\mathcal{P}}\hat{\mathbf{T}}\hat{\mathcal{P}} + \hat{\mathcal{P}}\hat{V}(\hat{\mathbf{x}})\hat{\mathcal{P}}. \tag{25}$$

Throughout this review, we use calligraphic symbols (such as $\hat{\mathcal{H}}_{\mathrm{M}}$) to indicate operators in the truncated Hilbert space.

TABLE I. Parameters used in the molecular Hamiltonian $\hat{H}_{\mathrm{M}}$.

Parameter	Model
$z_{\mathrm{p}}, z_{\mathrm{D}}, z_{\mathrm{A}}$	1 (unitless)
R_{D}	−3.5 Å
R_{A}	3.5 Å
R_{c}	1.75 Å
R_{n}	1.0 Å
m_{p}	1836 a.u.
m_{e}	1 a.u.

The simplest way to then write the QED Hamiltonians from Secs. II A and II B in this truncated subspace would then be to truncate each matter operator by $\hat{\mathcal{P}}$. Truncating the momentum operator and dipole operator as $\hat{\mathcal{P}}\hat{\mathbf{p}}_j\hat{\mathcal{P}}$ and $\hat{\mathcal{P}}\hat{\boldsymbol{\mu}}\hat{\mathcal{P}}$, the QED Hamiltonians under the truncated subspace are commonly defined as

$$\hat{\mathcal{H}}'_{\mathrm{p\cdot A}} = \hat{\mathcal{P}}\hat{U}^\dagger\hat{H}_{\mathrm{M}}\hat{U}\hat{\mathcal{P}} + \hat{H}_{\mathrm{ph}} = \hat{\mathcal{H}}_{\mathrm{M}} + \hat{H}_{\mathrm{ph}} + \sum_j\left(-\frac{z_j}{m_j}\hat{\mathcal{P}}\hat{\mathbf{p}}_j\hat{\mathcal{P}}\hat{\mathbf{A}} + \frac{z_j^2\hat{\mathbf{A}}^2}{2m_j}\right), \tag{26a}$$

$$\hat{\mathcal{H}}_{\mathrm{d\cdot E}} = \hat{\mathcal{H}}_{\mathrm{M}} + \hat{H}_{\mathrm{ph}} + i\omega_{\mathrm{c}}\hat{\mathcal{P}}\hat{\boldsymbol{\mu}}\hat{\mathcal{P}}\mathbf{A}_0(\hat{a}^\dagger - \hat{a}) + \frac{\omega_{\mathrm{c}}}{\hbar}(\hat{\mathcal{P}}\hat{\boldsymbol{\mu}}\hat{\mathcal{P}}\mathbf{A}_0)^2. \tag{26b}$$

Note that $\hat{\mathcal{H}}'_{\mathrm{p\cdot A}} = \hat{\mathcal{P}}\hat{H}_{\mathrm{p\cdot A}}\hat{\mathcal{P}} = \hat{\mathcal{P}}\hat{U}^\dagger\hat{H}_{\mathrm{M}}\hat{U}\hat{\mathcal{P}} + \hat{H}_{\mathrm{ph}}$. It is well known that the above two Hamiltonians do not generate the same polariton eigenspectrum[31,33,37,58–62] under the ultra-strong coupling regime,[28] explicitly breaking down the gauge invariance. This leads to the gauge ambiguity[33,63,64] as to which Hamiltonian, $\hat{\mathcal{H}}'_{\mathrm{p\cdot A}}$ or $\hat{\mathcal{H}}_{\mathrm{d\cdot E}}$, is viable to compute physical quantities when applying $\hat{\mathcal{P}}$. This is attributed[33,56] to the fact that $\hat{\mathcal{H}}'_{\mathrm{p\cdot A}}$ usually requires a larger subset of the matter states to converge or generate consistent results with $\hat{\mathcal{H}}_{\mathrm{d\cdot E}}$, and apparently, under the *complete* basis limit, they are gauge invariant [see Figs. 4(a)–4(d)]. Further, this fundamentally different behavior of $\hat{\mathcal{H}}'_{\mathrm{p\cdot A}}$ and $\hat{\mathcal{H}}_{\mathrm{d\cdot E}}$ upon state truncation is also attributed to the fundamental asymmetry of the operators $\hat{\mathbf{p}}$ and $\hat{\boldsymbol{\mu}} = \sum_j z_j\hat{\mathbf{x}}_j$.[33] This gauge ambiguity historically sources from the mid-20th century with studies on the two-level approximation for atom systems.[65] Figures 4(a)–4(d) show these convergence properties of both the dipole and Coulomb gauge Hamiltonians, demonstrating that for this Shin–Metiu model system,

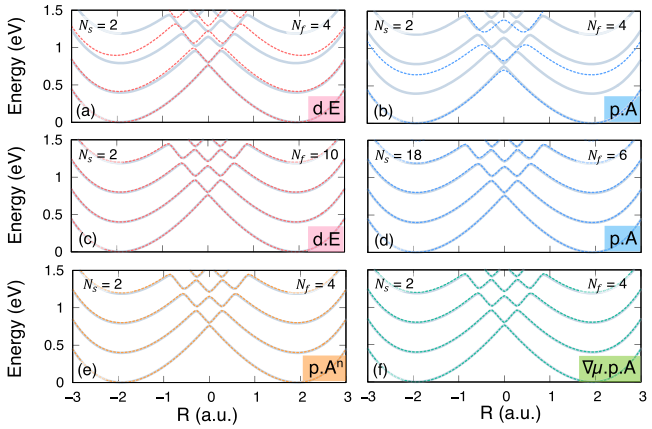

FIG. 4. Comparison of the polariton potential energy surfaces of the Shin–Metiu model generated from four different QED Hamiltonians under different levels of truncation for $A_0 = 0.15$ a.u. and $\omega_{\mathrm{c}} = 400$ meV. (a) Pauli–Fierz Hamiltonian with 2 matter states and 4 Fock states. (b) Coulomb gauge Hamiltonian with 2 matter states and 4 Fock states. (c) Pauli–Fierz Hamiltonian with 2 matter states and 10 Fock states. (d) Coulomb gauge Hamiltonian with 18 matter states and 6 Fock states. (e) Properly truncated Coulomb gauge Hamiltonian with 2 matter states and 4 Fock states. (f) Polarized Fock state (PFS) Hamiltonian with 2 matter states and 4 Fock states. This shows how the latter two Hamiltonians require less matter and Fock states to converge compared to the former two.

13 February 2025 02:07:04

Published under an exclusive license by AIP Publishing

$\hat{\mathcal{H}}'_{\text{p·A}}$ requires 9 times more matter states to converge [see Figs. 4(c) and 4(d)].

Performing the same truncation scheme, the PF Hamiltonian in the truncated electronic basis, $\hat{\mathcal{H}}_{\text{PF}} = \hat{U}_\theta \hat{\mathcal{H}}_{\text{d·E}} \hat{U}_\theta^\dagger = \hat{\mathcal{H}}_{\text{M}} + \hat{U}_\theta \hat{\mathcal{U}} \hat{H}_{\text{ph}} \hat{\mathcal{U}}^\dagger \hat{U}_\theta^\dagger$, is expressed as

$$\begin{aligned}\hat{\mathcal{H}}_{\text{PF}} &= \hat{\mathcal{H}}_{\text{M}} + \hat{H}_{\text{ph}} + \omega_{\text{c}} \hat{\mathcal{P}} \hat{\boldsymbol{\mu}} \hat{\mathcal{P}} \cdot \mathbf{A}_0 (\hat{a} + \hat{a}^\dagger) + \frac{\omega_{\text{c}}}{\hbar} (\hat{\mathcal{P}} \hat{\boldsymbol{\mu}} \hat{\mathcal{P}} \cdot \mathbf{A}_0)^2 \\ &= \hat{\mathcal{H}}_{\text{M}} + \frac{1}{2} \hat{p}_{\text{c}}^2 + \frac{1}{2} \omega_{\text{c}}^2 \left(\hat{q}_{\text{c}} + \sqrt{\frac{2}{\hbar \omega_{\text{c}}}} \hat{\mathcal{P}} \hat{\boldsymbol{\mu}} \hat{\mathcal{P}} \cdot \mathbf{A}_0 \right)^2 . \end{aligned} \tag{27}$$

Note that $\hat{U}_\theta$ is only a function of the photonic DOF, thus it does not bring any matter operator that was originally confined in $\hat{\mathcal{P}}$ to $\hat{\mathcal{Q}}$. Therefore, $\hat{\mathcal{H}}_{\text{PF}}$ provides consistent results with $\hat{\mathcal{H}}_{\text{d·E}}$, ensuring that there are no ambiguities between $\hat{\mathcal{H}}_{\text{d·E}}$ and $\hat{\mathcal{H}}_{\text{PF}}$.

C. Properly truncated Coulomb gauge Hamiltonian

Reference 36 contends that the gauge ambiguity between the Coulomb and dipole gauges emerges because the $\hat{\mathcal{P}}\hat{U}^\dagger$ and $\hat{U}\hat{\mathcal{P}}$ in $\hat{\mathcal{H}}'_{\text{p·A}}$ [Eq. (26a)] do not consistently constrain light–matter interaction operators in the same electronic subspace as do those corresponding operators in $\hat{\mathcal{H}}_{\text{d·E}}$. The source of this ambiguity lies in how much information of the full system is constrained in the subspace $\hat{\mathcal{P}}$ and how much is neglected upon truncation, center in the subspace $\hat{\mathcal{Q}} = \hat{\mathbb{1}}_{\text{r}} - \hat{\mathcal{P}}$, even when the matter eigenspectrum is converged for a truncation in $\hat{\mathcal{P}}$. Naturally, in the limit of $\hat{\mathcal{P}} \to \hat{\mathbb{1}}_{\text{r}}$, both $\hat{\mathcal{H}}'_{\text{p·A}}$ and $\hat{\mathcal{H}}_{\text{d·E}}$ have the same results, but in using $\hat{U}\hat{\mathcal{P}}$ to create $\hat{\mathcal{H}}'_{\text{p·A}}$, information on the light–matter coupling is cast into the subspace $\hat{\mathcal{Q}}$. Namely, the diamagnetic term $z_j^2 \hat{\boldsymbol{A}}^2 / 2m_j$ in $\hat{\mathcal{H}}'_{\text{p·A}}$ that is effectively evaluated in the full space[31,33] $\hat{\mathbb{1}}_{\text{r}}$ (based on the Thomas–Reiche–Kuhn sum rule), hence is not properly confined in $\hat{\mathcal{P}}$. As such, it overestimates its contribution in the subspace,[31,33] and by confining it within $\hat{\mathcal{P}}$, the results can be significantly improved.[31] Reference 36 proposes that the best way to confine the diamagnetic term to the projected subspace is to reformulate $\hat{U}$ as a unitary operator in said subspace. As such, using $\hat{\mathcal{P}}\hat{U}\hat{\mathcal{P}}$[31,58] does not resolve this gauge ambiguity either.

Based on the above conjecture, the gauge ambiguity in the truncated electronic subspace will be resolved by defining the following unitary operator:

$$\hat{\mathcal{U}} = \exp\left[-\frac{i}{\hbar} \hat{\mathcal{P}} \hat{\boldsymbol{\mu}} \hat{\mathcal{P}} \cdot \hat{\mathbf{A}} \right] \equiv \exp\left[-\frac{i}{\hbar} \tilde{\boldsymbol{\mu}}(\hat{\mathbf{x}}, \hat{\mathbf{p}}) \cdot \hat{\mathbf{A}} \right], \tag{28}$$

such that all terms in $\hat{\mathcal{U}} = \sum_{n=0}^{\infty} \frac{1}{n!} (-\frac{i}{\hbar})^n (\hat{\mathcal{P}} \hat{\boldsymbol{\mu}} \hat{\mathcal{P}})^n \hat{\mathbf{A}}^n$ are properly confined within the subspace $\hat{\mathcal{P}}$, and upon gauge transformation, all light–matter interaction operators are now consistently confined in $\hat{\mathcal{P}}$ for both gauges. Here, $\hat{\mathcal{U}}$ is defined analogously to the PZW gauge operator $\hat{U}$ in the full space [Eq. (5)], and $\hat{\mathcal{P}} \hat{\boldsymbol{\mu}} \hat{\mathcal{P}} \equiv \tilde{\boldsymbol{\mu}}(\hat{\mathbf{x}}, \hat{\mathbf{p}})$ in principle is a function of both $\hat{\mathbf{x}}$ and $\hat{\mathbf{p}}$, due to the finite level projection that ruins the locality of $\hat{\mathbf{x}}$.[31,66] Further, $\hat{\mathcal{U}}$ is a unitary transformation operator in the $\hat{\mathcal{P}}$ subspace and the identity operator in the subspace of $\hat{\mathbb{1}}_{\text{r}} - \hat{\mathcal{P}}$, such that we still have $\hat{\mathcal{U}}\hat{\mathcal{U}}^\dagger = \hat{\mathbb{1}}_{\text{r}} \otimes \hat{\mathbb{1}}_{\text{R}} \otimes \hat{\mathbb{1}}_{\text{ph}} = \hat{U}\hat{U}^\dagger$. Using $\hat{\mathcal{U}}$, one can define the following Coulomb gauge Hamiltonian:[36]

$$\hat{\mathcal{H}}_{\text{p·A}} = \hat{\mathcal{U}}^\dagger \hat{\mathcal{H}}_{\text{M}} \hat{\mathcal{U}} + \hat{H}_{\text{ph}}, \tag{29}$$

analogous to $\hat{H}_{\text{p·A}}$ in Eq. (6) in the full space. One can then formally show that $\hat{\mathcal{H}}_{\text{p·A}}$ [Eq. (29)] and $\hat{\mathcal{H}}_{\text{d·E}}$ [Eq. (26b)] are related through $\hat{\mathcal{U}}$ [Eq. (28)] as follows: $\hat{\mathcal{U}} \hat{\mathcal{H}}_{\text{p·A}} \hat{\mathcal{U}}^\dagger = \hat{\mathcal{H}}_{\text{M}} + \hat{\mathcal{U}} \hat{H}_{\text{ph}} \hat{\mathcal{U}}^\dagger = \hat{\mathcal{H}}_{\text{d·E}}$. Note that to establish the last equality, we have used the fact that $\hat{\mathcal{U}} \hat{H}_{\text{ph}} \hat{\mathcal{U}}^\dagger = \hat{\mathcal{U}} \left(\frac{1}{2} \omega_{\text{c}}^2 \hat{q}_{\text{c}}^2 + \frac{1}{2} \hat{p}_{\text{c}}^2 \right) \hat{\mathcal{U}}^\dagger = \frac{1}{2} \omega_{\text{c}}^2 \hat{q}_{\text{c}}^2 + \frac{1}{2} (\hat{p}_{\text{c}} + \sqrt{2\omega_{\text{c}}/\hbar} \hat{\mathcal{P}} \hat{\boldsymbol{\mu}} \hat{\mathcal{P}} \mathbf{A}_0)^2$. The unitary relation between $\hat{\mathcal{H}}_{\text{d·E}}$ and the new $\hat{\mathcal{H}}_{\text{p·A}}$ formally proves that there are no gauge ambiguities between these two gauges when following this truncation scheme.

While the above formulation is general and exact, it may not be immediately clear to the reader how to apply it. As such, we will walk through performing this truncation scheme for molecular QED, where the nuclear kinetic energy, $\hat{\mathbf{T}}_{\mathbf{R}}$ is typically separated from the electronic Hamiltonian $\hat{H}_{\text{el}} = \hat{H}_{\text{M}} - \hat{\mathbf{T}}_{\mathbf{R}}$. The *adiabatic* electronic states $|\alpha(\mathbf{R})\rangle$ are the eigenstates of $\hat{H}_{\text{el}}$ through $\hat{H}_{\text{el}} |\alpha(\mathbf{R})\rangle = (\hat{\mathbf{T}}_{\mathbf{r}} + \hat{V}) |\alpha(\mathbf{R})\rangle = E_\alpha(\mathbf{R}) |\alpha(\mathbf{R})\rangle$. Using $\hat{\mathcal{P}} = \sum_\alpha |\alpha(\mathbf{R})\rangle\langle\alpha(\mathbf{R})|$, the projected electronic Hamiltonian is $\hat{\mathcal{H}}_{\text{el}} = \hat{\mathcal{P}} \hat{H}_{\text{el}} \hat{\mathcal{P}} = \sum_\alpha E_\alpha(\mathbf{R}) |\alpha\rangle\langle\alpha|$. Alternatively, diabatic electronic states[67–70] $\{|\varphi\rangle, |\phi\rangle\}$ can be obtained by the unitary transform[67–71] from the adiabatic states $|\alpha(\mathbf{R})\rangle$. The character of the diabatic states do not depend on $\mathbf{R}$, such that $\langle\varphi|\nabla_{\mathbf{R}}|\phi\rangle = 0$. With $\hat{\mathcal{P}} = \sum_\varphi |\varphi\rangle\langle\varphi|$, $\hat{\mathcal{H}}_{\text{el}} = \hat{\mathcal{P}} \hat{H}_{\text{el}} \hat{\mathcal{P}} = \sum_\varphi \mathcal{V}_{\varphi\varphi}(\mathbf{R}) \times |\varphi\rangle\langle\varphi| + \sum_{\varphi \neq \phi} \mathcal{V}_{\varphi\phi}(\mathbf{R}) |\varphi\rangle\langle\phi|$, where $\mathcal{V}_{\varphi\phi}(\mathbf{R}) = \langle\varphi|\hat{H}_{\text{el}}|\phi\rangle$ is a diabatic matrix element of $\hat{H}_{\text{el}}$.

By splitting the matter Hamiltonian as $\hat{H}_{\text{M}} = \hat{\mathbf{T}}_{\mathbf{R}} + \hat{H}_{\text{el}}$, then the resulting molecular QED Hamiltonian in this gauge is

$$\begin{aligned}\hat{\mathcal{H}}_{\text{p·A}} &= \hat{\mathcal{U}}^\dagger \hat{\mathcal{P}} \hat{\mathbf{T}}_R \hat{\mathcal{P}} \hat{\mathcal{U}} + \hat{\mathcal{U}}^\dagger \hat{\mathcal{P}} \hat{H}_{\text{el}}(\hat{\mathbf{p}}_r, \hat{\mathbf{x}}) \hat{\mathcal{P}} \hat{\mathcal{U}} + \hat{H}_{\text{ph}} \\ &= \sum_{j \in R} \frac{1}{2m_j} \hat{\mathcal{P}} (\hat{\mathbf{p}}_j - \nabla_j \tilde{\boldsymbol{\mu}} \hat{\mathbf{A}} + \tilde{\mathbf{P}}_j)^2 \hat{\mathcal{P}} + \hat{\mathcal{U}}^\dagger \hat{\mathcal{H}}_{\text{el}} \hat{\mathcal{U}} + \hat{H}_{\text{ph}}, \end{aligned} \tag{30}$$

where the sum over j *only* includes nuclei, $\tilde{\boldsymbol{\mu}} \equiv \hat{\mathcal{P}} \hat{\boldsymbol{\mu}} \hat{\mathcal{P}}$, and $\tilde{\mathbf{P}}_j$ represents the residue momentum $\tilde{\mathbf{P}}_j \equiv \frac{1}{2} (\frac{i}{\hbar})^2 [\tilde{\boldsymbol{\mu}} \hat{\mathbf{A}}, [\tilde{\boldsymbol{\mu}} \hat{\mathbf{A}}, \hat{\mathbf{p}}_j]] + \cdots$. In the above expression, we did not specify the choice of $\hat{\mathcal{P}}$, which could be either adiabatic or diabatic. Under the limiting case when $\mathbf{A}_0 = 0$ or $\tilde{\boldsymbol{\mu}} \cdot \hat{\mathbf{A}} = 0$, both the $-\nabla_j \tilde{\boldsymbol{\mu}} \hat{\mathbf{A}}$ and $\tilde{\mathbf{P}}_j$ terms become 0, and $\hat{\mathcal{U}}^\dagger = \hat{\mathcal{U}} \to \hat{\mathcal{P}} \otimes \hat{\mathbb{1}}_{\text{R}} \otimes \hat{\mathbb{1}}_{\text{ph}}$. As one would expect, the zero-coupling limit returns to just the addition of the two DOFs, $\hat{\mathcal{H}}_{\text{p·A}} \to \hat{\mathcal{H}}_{\text{M}} + \hat{H}_{\text{ph}}$.

When using adiabatic states for the truncation, one can show that[70,72] $\hat{\mathcal{P}} \hat{\mathbf{p}}_j^2 \hat{\mathcal{P}} = (\hat{\mathbf{p}}_j - i\hbar \sum_{\alpha,\beta} \mathbf{d}^j_{\alpha\beta} |\alpha\rangle\langle\beta|)^2$, where $\mathbf{d}^j_{\alpha\beta} \equiv \langle\alpha|\nabla_j|\beta\rangle$ are the well-known derivative couplings. In addition to these adiabatic derivative couplings, the light–matter interaction also induced additional "derivative"-type couplings, $-\nabla_j \tilde{\boldsymbol{\mu}} \hat{\mathbf{A}}$ and $\tilde{\mathbf{P}}_j$.

When using the Mulliken–Hush diabatic states,[68,73] which are the eigenstates of the $\tilde{\boldsymbol{\mu}} \equiv \hat{\mathcal{P}} \hat{\boldsymbol{\mu}} \hat{\mathcal{P}}$ operator, such that $\tilde{\boldsymbol{\mu}} = \sum_\phi \boldsymbol{\mu}_\phi |\phi\rangle\langle\phi|$, one can prove that $\tilde{\mathbf{P}}_j = 0$ for all nuclei. This is because that $\nabla_j \tilde{\boldsymbol{\mu}} = \sum_\phi \nabla_j \boldsymbol{\mu}_\phi |\phi\rangle\langle\phi|$, thus both $\tilde{\boldsymbol{\mu}} \hat{\mathbf{A}}$ and $[\tilde{\boldsymbol{\mu}} \hat{\mathbf{A}}, \hat{\mathbf{p}}_j]$ become purely diagonal matrices, hence all of the higher order commutators in

13 February 2025 02:07:04

Published under an exclusive license by AIP Publishing

$\hat{\mathcal{U}}^\dagger \hat{\mathbf{p}}_j \hat{\mathcal{U}}$ become zero, resulting in $\tilde{\mathbf{P}}_j = 0$ for $j \in \mathbf{R}$. This is analogous to the diabatization criteria for pure matter systems, where $\mathbf{d}^j_{\phi\varphi} = 0$, furthering the analogy of $\nabla_j \tilde{\boldsymbol{\mu}} \hat{\mathbf{A}}$ and $\tilde{\mathbf{P}}_j$ being similar to a derivative coupling.

This scheme of properly truncating the matter DOF thus yields gauge invariant results for this matter truncation, regardless of the matter basis. Additionally, it preserves the favorable Fock state convergence behavior of the Coulomb gauge Hamiltonian. Consequently, it requires fewer matter and Fock states than either of the Hamiltonians discussed above. This convergence behavior is demonstrated numerically in Fig. 4(e) for the Shin–Metiu molecular model.

D. Polarized Fock-state Hamiltonian

The polarized Fock-state Hamiltonian takes advantage of the disappearance of $\tilde{\mathbf{P}}_j$ when the Hamiltonian is expressed in the Mulliken–Hush diabatic basis to form an equivalent Hamiltonian that provides additional physical intuition. In the Mulliken–Hush diabatic basis, the matter Hamiltonian is expressed as

$$\hat{\mathcal{H}}_{\mathrm{M}} = \hat{\mathbf{T}}_{\mathbf{R}} + \sum_{\phi} V_{\phi}(\mathbf{R})|\phi\rangle\langle\phi| + \sum_{\phi\neq\varphi} V_{\phi\varphi}(\mathbf{R})|\phi\rangle\langle\varphi|, \tag{31}$$

where $V_\phi(\mathbf{R})$ represents the diabatic potentials, $V_{\phi\varphi}(\mathbf{R})$ represents the diabatic coupling. The PF Hamiltonian in Eq. (10) under the $|\phi\rangle$ basis is expressed as

$$\begin{aligned}\hat{\mathcal{H}}^{\mathrm{MH}}_{\mathrm{PF}} &= \hat{\mathcal{U}}^\dagger_\mu \hat{\mathcal{H}}_{\mathrm{PF}} \hat{\mathcal{U}}_\mu \\ &= \hat{H}_{\mathrm{M}} + \frac{\hat{p}_{\mathrm{c}}^2}{2} + \sum_{\phi} \frac{\omega_{\mathrm{c}}^2}{2}(\hat{q}_{\mathrm{c}} + q^0_\phi(\mathbf{R})|\phi\rangle\langle\phi|)^2,\end{aligned} \tag{32}$$

where $q^0_\phi(\mathbf{R}) = \sqrt{\frac{2}{\hbar\omega_{\mathrm{c}}}}\mathbf{A_0}\cdot\boldsymbol{\mu}_\phi(\mathbf{R})$, $\boldsymbol{\mu}_\phi$ is eigen-dipole value for $|\phi\rangle$, and $\hat{\mathcal{U}}_\mu$ is the unitary operator that changes the basis to the eigenbasis of $\hat{\boldsymbol{\mu}}$. In this representation, the photonic DOF is simply a displaced harmonic oscillator centered about $-q^0_\phi(\mathbf{R})$. This displacement can be viewed as a *polarization* of the photon field due to the presence of the molecule-cavity coupling, such that the photon field corresponds to a non-zero (hence polarized) vector potential, in contrast to the vacuum photon field.

We can then rewrite this displaced harmonic oscillator term in Eq. (32) in its own Fock basis, diagonalizing it as

$$\begin{aligned}&\frac{1}{2}\left[\hat{p}_{\mathrm{c}}^2 + \omega_{\mathrm{c}}^2(\hat{q}_{\mathrm{c}} + q^0_\phi(\mathbf{R}))^2\right]|n_\phi(\mathbf{R})\rangle \\ &\quad\equiv \left(\hat{b}^\dagger_\phi \hat{b}_\phi + \frac{1}{2}\right)\hbar\omega_{\mathrm{c}}|n_\phi(\mathbf{R})\rangle = \left(n_\phi + \frac{1}{2}\right)\hbar\omega_{\mathrm{c}}|n_\phi(\mathbf{R})\rangle,\end{aligned} \tag{33}$$

where the polarized Fock state (PFS) $|n_\phi(\mathbf{R})\rangle \equiv |n_\phi\rangle$ is the Fock state of a displaced Harmonic oscillator, with the displacement $-q^0_\phi = -\sqrt{\frac{2}{\hbar\omega_{\mathrm{c}}}}\mathbf{A_0}\cdot\boldsymbol{\mu}_\phi(\mathbf{R})$ specific to the diabatic state $|\phi\rangle$ such that $|n_\phi\rangle = e^{-i(-q^0_\phi)\hat{p}/\hbar}|n\rangle = e^{iq^0_\phi\hat{p}/\hbar}|n\rangle$, and $n_\phi = 0, 1, 2\ldots, \infty$ is the quantum number for the PFS. Further, $\hat{b}^\dagger_\phi = (\hat{q}'_\phi + i\hat{p})/\sqrt{2}$ and $\hat{b}_\phi = (\hat{q}'_\phi - i\hat{p})/\sqrt{2}$ are the creation and annihilation operators of the PFS $|n_\phi\rangle$, with the photon field momentum operator $\hat{p}$ and polarized photon field coordinate operator $\hat{q}'_\phi = \hat{q} + q^0_\phi(\mathbf{R})$. Note that in contrast to a noninteracting photonic system, the PFS $\boldsymbol{\mu}_\phi(\mathbf{R})$ has an explicit dependence on the eigen-dipole of the molecule for each given nuclear coordinate. As such PFS's corresponding to different MH diabats are not in general, orthogonal, i.e., $\langle n_\phi|m_\varphi\rangle \neq \delta_{\phi\varphi}$ Under the special case of the atomic cavity QED, the PFS representation reduces to the qubit-shifted Fock basis $\{|n_+\rangle, |m_-\rangle\}$, which has been used to solve the polariton eigen-spectrum for the quantum Rabi model[74–77] throughout the range of light–matter coupling and to derive the generalized rotating-wave approximation.[74,75,78] These non-orthogonal Fock states and their overlap $\langle m_-|n_+\rangle$ have shown to effectively capture the light–matter interactions in a quantum Rabi model.[74,75]

To express the full light–matter Hamiltonian in the PFS representation, the PF Hamiltonian [Eq. (32)] undergoes a unitary shift operator (similar to a polaron transformation[15]) $\hat{\mathcal{U}}_{\mathrm{pol}}$ of the form

$$\hat{\mathcal{U}}_{\mathrm{pol}} = \exp\left[\frac{i}{\hbar}\sum_{\phi} q^0_\phi(\mathbf{R})|\phi\rangle\langle\phi|\hat{p}_c\right], \tag{34}$$

such that it unshifts that displaced Harmonic oscillator in Eq. (32) when applied to $\hat{H}_{\mathrm{PF}}$. Note that this is also similar to the coherent state transformation[49,79–100] or the Lang–Firsov transformation[79,88,89,101] that are used in *ab initio* QED calculations; however, for the purpose of those calculations, the matter DOF is not represented in the Mulliken–Hush basis, and the general form of $\hat{\boldsymbol{\mu}}$ is used instead of the matrix elements, q^0_ϕ. Consequently, these *ab initio* techniques also show the same computational advantages for the photonic DOF as PFS but solve the matter DOF self-consistently.

Upon the transformation by $\hat{\mathcal{U}}_{\mathrm{pol}}$, we then have the PFS Hamiltonian as

$$\begin{aligned}\hat{\mathcal{H}}_{\mathrm{PFS}} &= \hat{\mathcal{U}}^\dagger_{\mathrm{pol}}\hat{\mathcal{H}}^{\mathrm{MH}}_{\mathrm{PF}}\hat{\mathcal{U}}_{\mathrm{pol}} \\ &= \hat{\mathcal{U}}^\dagger_{\mathrm{pol}}\hat{\mathbf{T}}_{\mathbf{R}}\hat{\mathcal{U}}_{\mathrm{pol}} + \sum_{\phi,n_\phi}\left(V_\phi(\mathbf{R}) + \left(n_\phi + \frac{1}{2}\right)\hbar\omega_{\mathrm{c}}\right)|\phi, n_\phi\rangle\langle n_\phi, \phi| \\ &\quad + \sum_{n_\phi, m_\varphi, \phi\neq\varphi}\langle m_\varphi|n_\phi\rangle V_{\phi\varphi}(\mathbf{R})|\phi, n_\phi\rangle\langle m_\varphi, \varphi|.\end{aligned} \tag{35}$$

In contrast to other representations such as those discussed in Sec. II, this Hamiltonian does not have an explicit light–matter interaction term. Instead, all interactions are mediated via the overlap of the shifted Fock states through the $\langle m_\varphi|n_\phi\rangle V_{\phi\varphi}(\mathbf{R})$ term and the $\hat{\mathcal{U}}^\dagger_{\mathrm{pol}}\hat{\mathbf{T}}_{\mathbf{R}}\hat{\mathcal{U}}_{\mathrm{pol}}$ term.

We can further express the $\hat{\mathcal{U}}^\dagger_{\mathrm{pol}}\hat{\mathbf{T}}_{\mathbf{R}}\hat{\mathcal{U}}_{\mathrm{pol}}$ term in the $|\phi, n_\phi\rangle$ basis as

$$\hat{\mathcal{U}}^\dagger_{\mathrm{pol}}\hat{\mathbf{T}}_{\mathbf{R}}\hat{\mathcal{U}}_{\mathrm{pol}} = \frac{1}{2\mathbf{M}}\left(\hat{\mathbf{P}} - i\hbar\sum_{\phi,n_\phi,m_\phi}\mathbf{d}_{m_\phi n_\phi}|\phi, m_\phi\rangle\langle n_\phi, \phi|\right)^2, \tag{36}$$

where $\mathbf{d}_{m_\phi n_\phi} = \langle m_\phi|\nabla_{\mathbf{R}}|n_\phi\rangle$ originates from the R-dependence of PFS. Note that there is no non-adiabatic couplings between states with different diabatic characters, since $\langle\phi, n_\phi|\nabla_{\mathbf{R}}|\varphi, m_\varphi\rangle = \langle n_\phi|\nabla_{\mathbf{R}}|m_\varphi\rangle\langle\phi|\varphi\rangle = 0$ (because we assume that $|\phi\rangle$ and $|\varphi\rangle$ are strict diabatic basis), and they are orthogonal $\langle\phi|\varphi\rangle = 0$ for $\phi \neq \varphi$. The polaritonic non-adiabatic coupling can be analytically evaluated as follows:

$$\langle m_\phi|\nabla_{\mathbf{R}}|n_\phi\rangle = -\frac{1}{\hbar}\mathbf{A_0}\cdot\nabla_{\mathbf{R}}\boldsymbol{\mu}_\phi(\mathbf{R})\langle\mathbf{m}_\phi|\hat{\mathbf{b}}^\dagger - \hat{\mathbf{b}}|\mathbf{n}_\phi\rangle. \tag{37}$$

13 February 2025 02:07:04

Published under an exclusive license by AIP Publishing

Thus, these terms couple off-resonant states that are separated by $\hbar\omega_c$ through the $(\hat{b}^\dagger - \hat{b})$ term. This non-adiabatic coupling is reminiscent of the vector potential boost of matter momentum in the Coulomb gauge.

Intuitively, this PFS representation strives to improve the Fock state convergence of the d · E Hamiltonian by using a shifted harmonic oscillator basis instead of the traditional Fock basis of the pure light Hamiltonian. This is because the light–matter coupling itself causes a shift in the photonic Hamiltonian [as shown in Eq. (33)]. Thus, a shifted harmonic oscillator basis is a more natural basis in which to represent this system. This leads to a significant improvement in Fock state convergence over the d·E Hamiltonian, as shown numerically in Fig. 4. Additionally, Fig. 5 shows in further detail the advantageous convergence properties of the PFS representation compared to $\hat{\mathcal{H}}_{\text{d·E}}$ and $\hat{\mathcal{H}}'_{\text{p·A}}$.

In fact, this PFS representation is equivalent to the properly truncated Coulomb gauge Hamiltonian in Eq. (30). To see this, we first look at how $\hat{U}_\theta$ rotates $\hat{q}_c$,

$$\hat{U}_\theta^\dagger \hat{q}_c \hat{U}_\theta = \sqrt{\frac{\hbar}{2\omega_c}}(\hat{U}_\theta^\dagger \hat{a} \hat{U}_\theta + \hat{U}_\theta^\dagger \hat{a}^\dagger \hat{U}_\theta) = -\frac{\hat{p}_c}{\omega_c}. \tag{38}$$

This relation directly leads to

$$\begin{aligned}\hat{\mathcal{U}}_\mu^\dagger \hat{U}_\theta^\dagger \hat{\mathcal{U}} \hat{U}_\theta \hat{\mathcal{U}}_\mu &= \hat{\mathcal{U}}_\mu^\dagger \hat{U}_\theta^\dagger \exp\left[-\frac{i}{\hbar}\sqrt{\frac{2\omega_c}{\hbar}}\hat{\boldsymbol{\mu}} \cdot \mathbf{A}_0 \hat{q}_c\right] \hat{U}_\theta \hat{\mathcal{U}}_\mu \\ &= \hat{\mathcal{U}}_\mu^\dagger \exp\left[\frac{i}{\hbar}\sqrt{\frac{2}{\hbar\omega_c}}\hat{\boldsymbol{\mu}} \cdot \mathbf{A}_0 \hat{p}_c\right] \hat{\mathcal{U}}_\mu \\ &= \exp\left[\frac{i}{\hbar}\sum_\phi \sqrt{\frac{2}{\hbar\omega_c}}\boldsymbol{\mu}_\phi \cdot \mathbf{A}_0 |\phi\rangle\langle\phi|\hat{p}_c\right] = \hat{U}_{\text{pol}}. \end{aligned} \tag{39}$$

With the properties shown in Eqs. (38) and (40), we can directly show that $\hat{\mathcal{H}}_{\text{PFS}}$ and $\hat{\mathcal{H}}_{\text{p·A}}$ differ only by a change in basis for the matter Hilbert space and a phase rotation in the photonic Hilbert space by the following relationship:

$$\begin{aligned}\hat{\mathcal{H}}_{\text{PFS}} &= \hat{\mathcal{U}}_{\text{pol}}^\dagger \hat{\mathcal{H}}_{\text{PF}}^{\text{MH}} \hat{\mathcal{U}}_{\text{pol}} = \hat{\mathcal{U}}_{\text{pol}}^\dagger (\hat{\mathcal{U}}_\mu^\dagger \hat{\mathcal{H}}_{\text{PF}} \hat{\mathcal{U}}_\mu) \hat{\mathcal{U}}_{\text{pol}} \\ &= \hat{\mathcal{U}}_{\text{pol}}^\dagger \left(\hat{\mathcal{U}}_\mu^\dagger \left[\hat{U}_\theta^\dagger \hat{\mathcal{H}}_{\text{d·E}} \hat{U}_\theta\right] \hat{\mathcal{U}}_\mu\right) \hat{\mathcal{U}}_{\text{pol}} \\ &= (\hat{\mathcal{U}}_\mu^\dagger \hat{U}_\theta^\dagger \hat{\mathcal{U}}^\dagger \hat{U}_\theta \hat{\mathcal{U}}_\mu)\left(\hat{\mathcal{U}}_\mu^\dagger \left[\hat{U}_\theta^\dagger \hat{\mathcal{H}}_{\text{d·E}} \hat{U}_\theta\right] \hat{\mathcal{U}}_\mu\right)(\hat{\mathcal{U}}_\mu^\dagger \hat{U}_\theta^\dagger \hat{\mathcal{U}} \hat{U}_\theta \hat{\mathcal{U}}_\mu) \\ &= \hat{\mathcal{U}}_\mu^\dagger \hat{U}_\theta^\dagger \hat{\mathcal{U}}^\dagger \hat{\mathcal{H}}_{\text{d·E}} \hat{\mathcal{U}} \hat{U}_\theta \hat{\mathcal{U}}_\mu \\ &= \hat{\mathcal{U}}_\mu^\dagger \hat{U}_\theta^\dagger \hat{\mathcal{H}}_{\text{p·A}} \hat{U}_\theta \hat{\mathcal{U}}_\mu. \end{aligned} \tag{40}$$

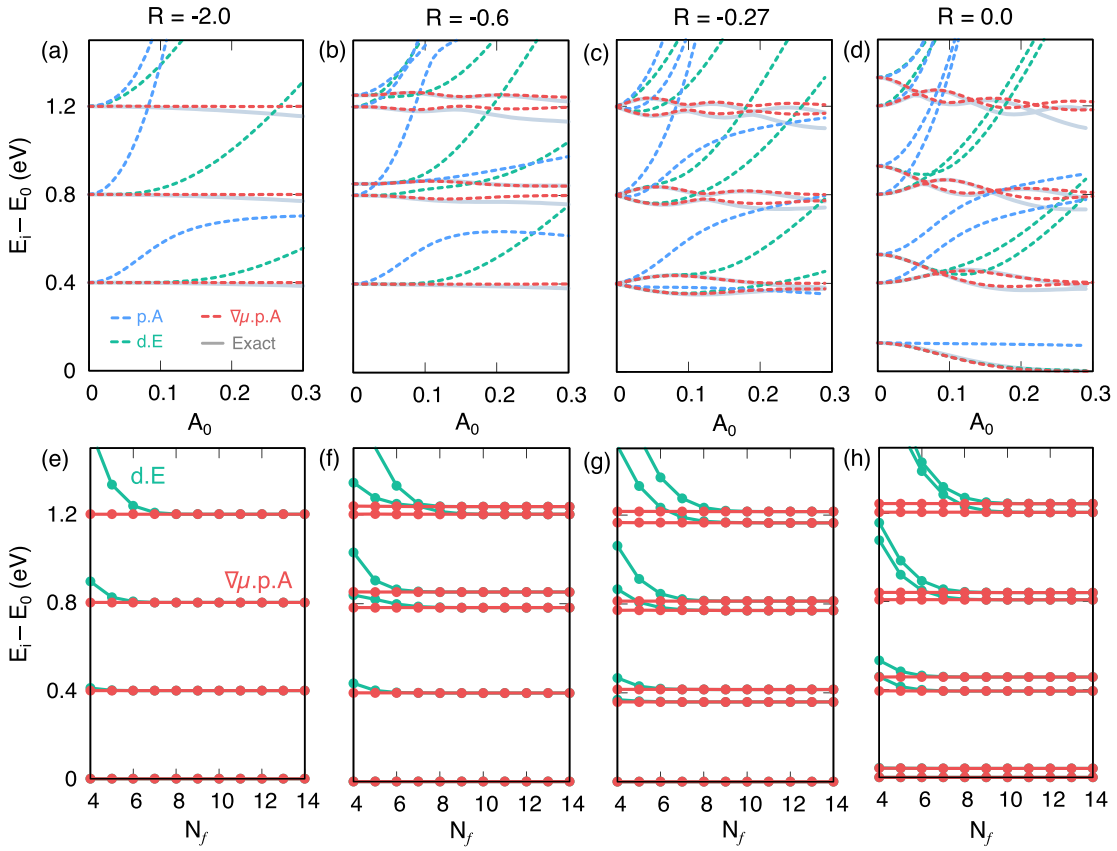

FIG. 5. Comparison of the PFS Hamiltonian (red) energy eigenspectrum with that of the Coulomb (blue) and dipole (green) gauge Hamiltonians ($\omega_c = 400$ meV) for the Shin–Metiu model at different R values (denoted at the top of each column). The top panels (a–d) graph the eigenenergies of each Hamiltonian using 2 matter states and 4 Fock states against the exact (gray). The bottom panels (e–h) plot the eigenenergies of the dipole gauge Hamiltonian vs the PFS Hamiltonian at different R values with an $A_0 = 0.15$ and two matter states as a function of the number of Fock states used.

13 February 2025 02:07:04

Published under an exclusive license by AIP Publishing

Note that $[\hat{U}_{\theta}, \hat{\mathcal{U}}_{\mu}] = 0$ since they act on different degrees of freedom. In this way, $\hat{\mathcal{H}}_{\text{PFS}}$ and $\hat{\mathcal{H}}_{\text{p·A}}$ are intrinsically related. It follows naturally that they would have very similar convergence properties. Consequentially, in the full basis limit, the PFS representation is equivalent to the p A Hamiltonian. This is shown in Sec. III E.

Figure 2 summarizes the relationships between all the Hamiltonians discussed thus far.

E. Truncation of the photonic mode for the Coulomb and dipole gauges

All the Hamiltonians previously discussed in this review are under the single mode approximation; however, many types of cavities such as the Fabry–Pérot cavity has infinite number of quantized modes (see Sec. VI). It is then pertinent to consider how to truncate this many-mode Hilbert space to a more computable space with a small finite number of modes. Whenever a truncation occurs, the gauge invariance condition may become ambiguous.

Although less ubiquitous than the gauge ambiguities present under matter truncation, it should be noted that the truncation of photonic modes also leads to gauge ambiguities that can be resolved in a manner similar to the process discussed in Sec. III C.[102] However, unlike in the case of matter truncation, for mode truncation, the dipole gauge Hamiltonian leads to ambiguities. To see this, recall how $\hat{H}_{\text{p·A}}$ and $\hat{H}_{\text{d·E}}$ can be written in terms of the PZW operator:

$$\hat{H}_{\text{p·A}} = \hat{U}^{\dagger}\hat{H}_{\text{M}}\hat{U} + \hat{H}_{\text{ph}}, \tag{41}$$

$$\hat{H}_{\text{d·E}} = \hat{H}_{\text{M}} + \hat{U}\hat{H}_{\text{ph}}\hat{U}^{\dagger}. \tag{42}$$

However, now $\hat{H}_{\text{ph}} = \sum_{k=0}^{\infty}\hbar\omega_k\hat{a}_k^{\dagger}\hat{a}_k$, where $\hat{a}_k$ is the photonic annihilation operator for the kth mode.

It is convenient to define a projection operator, $\hat{\mathcal{P}}^{(m)}$, that truncates this many-mode Hilbert space to an m-mode Hilbert space:

$$\hat{\mathcal{P}}^{(m)} = \hat{\mathcal{I}}_{\text{M}} \otimes \left(\bigotimes_{k=0}^{m-1}\sum_{n=0}^{\infty}|n_k\rangle\langle n_k| \bigotimes_{k'=m}^{\infty}|0_{k'}\rangle\langle 0_{k'}|\right), \tag{43}$$

where $|n_k\rangle$ is the nth Fock state in the kth mode and $\hat{\mathcal{I}}_M$ is the identity operator for the matter Hilbert space.

For the case of matter truncation, it was argued that to properly truncate polariton systems in a truncated subspace, the pure matter and photonic operators should be truncated first and then transformed with a properly truncated PZW operator. As discussed in Ref. 102, the same procedure must be used for mode truncation. In this manner, the new m-mode PZW operator is

$$\hat{\mathcal{U}}^{(m)} = e^{-\frac{i}{\hbar}\hat{\mathcal{P}}^{(m)}(\hat{\boldsymbol{\mu}}\cdot\hat{\mathbf{A}})\hat{\mathcal{P}}^{(m)}} = \exp\left[-\frac{i}{\hbar}\hat{\boldsymbol{\mu}}\cdot\sum_{k=0}^{m-1}\boldsymbol{A}_k(\hat{a}_k^{\dagger}+\hat{a}_k)\right]. \tag{44}$$

If we formulate the equivalents to Eqs. (41) and (42) in this m-mode subspace as

$$\hat{\mathcal{H}}_{\text{p·A}} = \hat{\mathcal{U}}^{\dagger}\hat{\mathcal{P}}\hat{H}_{\text{M}}\hat{\mathcal{P}}\hat{\mathcal{U}} + \hat{\mathcal{P}}\hat{H}_{\text{ph}}\hat{\mathcal{P}}, \tag{45}$$

$$\hat{\mathcal{H}}_{\text{d·E}} = \hat{\mathcal{P}}\hat{H}_{\text{M}}\hat{\mathcal{P}} + \hat{\mathcal{U}}\hat{\mathcal{P}}\hat{H}_{\text{ph}}\hat{\mathcal{P}}\hat{\mathcal{U}}^{\dagger}, \tag{46}$$

which always guarantees gauge invariant results through $\hat{\mathcal{H}}_{\text{d·E}} = \hat{\mathcal{U}}\hat{\mathcal{H}}_{\text{p·A}}\hat{\mathcal{U}}^{\dagger}$. We can find the Coulomb gauge Hamiltonian under an m-mode truncation by using Eq. (45)

$$\begin{aligned}\hat{\mathcal{H}}_{\text{p·A}}^{(m)} &= \hat{\mathcal{U}}^{(m)\dagger}\hat{\mathcal{P}}^{(m)}\hat{H}_{\text{M}}\hat{\mathcal{P}}^{(m)}\hat{\mathcal{U}}^{(m)} + \hat{\mathcal{P}}^{(m)}\sum_{k=0}^{\infty}\hbar\omega_k\hat{a}_k^{\dagger}\hat{a}_k\hat{\mathcal{P}}^{(m)}\\ &= \hat{H}_{\text{M}} + \sum_{k=0}^{m-1}\left[\hbar\omega_k\hat{a}_k^{\dagger}\hat{a}_k + \frac{\hat{\mathbf{p}}\cdot\mathbf{A}_k}{m}(\hat{a}_k^{\dagger}+\hat{a}_k)\right]\\ &\quad + \frac{1}{2m}\left[\sum_{k=0}^{m-1}|\mathbf{A}_k|(\hat{a}_k^{\dagger}+\hat{a}_k)\right]^2.\end{aligned} \tag{47}$$

Since $\hat{H}_{\text{M}}$ is a pure matter operator, it is invariant upon mode truncation and therefore commutes with $\hat{\mathcal{P}}$, $\hat{\mathcal{P}}^{(m)}\hat{H}_{\text{M}}\hat{\mathcal{P}}^{(m)} = \hat{H}_{\text{M}}\hat{\mathcal{P}}^{(m)}$. In the case of a single mode $m = 1$, Eq. (47) reduces to the well-known single-mode minimal coupling Hamiltonian [see Eq. (4)]. Interestingly, if we apply a simple mode truncation, $\hat{\mathcal{H}}_{\text{p·A}}^{\prime(m)} = \hat{\mathcal{P}}^{(m)}\hat{H}_{\text{p·A}}\hat{\mathcal{P}}^{(m)}$ has the same form of Eq. (47) up to a constant that represents the zero-point energy of all modes.

Since the minimal coupling Hamiltonian is formed by boosting the matter Hamiltonian, a naive mode truncation has a minimal effect, only causing a zero-point energy (ZPE) shift.

$$\begin{aligned}\hat{\mathcal{H}}_{\text{p·A}}^{\prime(m)} &= \hat{\mathcal{P}}^{(m)}\hat{H}_{\text{p·A}}\hat{\mathcal{P}}^{(m)}\\ &= \hat{\mathcal{P}}^{(m)}\hat{U}^{\dagger}\hat{H}_{\text{M}}\hat{U}\hat{\mathcal{P}}^{(m)} + \hat{\mathcal{P}}^{(m)}\sum_{k=0}^{\infty}\hbar\omega_k\hat{a}_k^{\dagger}\hat{a}_k\hat{\mathcal{P}}^{(m)}\\ &= \hat{H}_{\text{M}} + \sum_{k=0}^{m-1}\left[\hbar\omega_k\hat{a}_k^{\dagger}\hat{a}_k + \frac{\hat{\boldsymbol{p}}\cdot\boldsymbol{A}_k}{m}(\hat{a}_k^{\dagger}+\hat{a}_k)\right]\\ &\quad + \frac{1}{2m}\left[\sum_{k=0}^{m-1}|\boldsymbol{A}_k|(\hat{a}_k^{\dagger}+\hat{a}_k)\right]^2 + \mathcal{E}\hat{\mathcal{P}}^{(m)},\end{aligned} \tag{48}$$

where $\mathcal{E} = \sum_{k=n}^{\infty}|\boldsymbol{A}_k|^2/2m$ is ZPE of the other projected modes coming from $\hat{\mathcal{P}}^{(m)}(\hat{a}_k^{\dagger}+\hat{a}_k)^2\hat{\mathcal{P}}^{(m)} = \hat{\mathcal{P}}^{(m)}$ for $k \geq m$ (note that the only surviving term is $\hat{\mathcal{P}}^{(m)}\hat{a}_k\hat{a}_k^{\dagger}\hat{\mathcal{P}}^{(m)} = \hat{\mathcal{P}}^{(m)}$). This is very different from what happens in the case of a matter truncation.

Now, the Hamiltonian that fails under a simple mode truncation is the dipole gauge Hamiltonian.

$$\begin{aligned}\hat{\mathcal{H}}_{\text{d·E}}^{\prime(m)} &= \hat{\mathcal{P}}^{(m)}\hat{H}_{\text{d·E}}\hat{\mathcal{P}}^{(m)}\\ &= \hat{H}_{\text{M}} + \hat{\mathcal{P}}^{(m)}\hat{U}\left(\sum_{k=0}^{\infty}\hbar\omega_k\hat{a}_k^{\dagger}\hat{a}_k\right)\hat{U}^{\dagger}\hat{\mathcal{P}}^{(m)}\\ &= \hat{H}_{\text{M}} + \sum_{k=0}^{m-1}\left[\hbar\omega_k\hat{a}_k^{\dagger}\hat{a}_k + i\omega_k\boldsymbol{A}_k\cdot\hat{\boldsymbol{\mu}}(\hat{a}_k^{\dagger}-\hat{a}_k)\right]\\ &\quad + \sum_{k=0}^{\infty}\frac{\omega_k}{\hbar}(\boldsymbol{A}_k\cdot\hat{\boldsymbol{\mu}})^2.\end{aligned} \tag{49}$$

This procedure breaks the gauge invariance and generate different results from $\hat{\mathcal{H}}_{\text{p·A}}^{(m)}$, because the dipole self-energies for all the modes are still explicitly present, even for the modes $k \in [m, \infty]$, which are supposed to be projected away. Thus, the dipole gauge Hamiltonian should be truncated using the scheme presented in Eq. (46),

13 February 2025 02:07:04

Published under an exclusive license by AIP Publishing

$$\hat{\mathcal{H}}^{(m)}_{\mathrm{d.E}} = \hat{H}_{\mathrm{M}} + \hat{\mathcal{U}}^{(m)}\hat{\mathcal{P}}^{(m)}\left(\sum_{k=0}^{\infty}\hbar\omega_k\hat{a}_k^\dagger\hat{a}_k\right)\hat{\mathcal{P}}^{(m)}\hat{\mathcal{U}}^{(m)\dagger}$$
$$= \hat{H}_{\mathrm{M}} + \sum_{k=0}^{n-1}\left[\hbar\omega_k\hat{a}_k^\dagger\hat{a}_k + i\omega_k\boldsymbol{A}_k\cdot\hat{\boldsymbol{\mu}}(\hat{a}_k^\dagger - \hat{a}_k) + \frac{\omega_k}{\hbar}(\boldsymbol{A}_k\cdot\hat{\boldsymbol{\mu}})^2\right]. \tag{50}$$

This provides gauge invariant results with Eq. (48) and reduces to the well-known single mode case [see Eq. (7)] when $m = 1$. In this manner, one should carefully consider the proper manner of truncation even for mode truncation.

F. Generalization of truncation scheme beyond the long-wavelength approximation

In a recent work,[43] a generalized scheme for resolving gauge ambiguities beyond the long-wavelength approximation and for arbitrary gauges. In this picture, the matter is no longer approximated as a dipole and instead must be described as a charge density function, $\rho(\mathbf{x})$,

$$\hat{\rho}(\mathbf{x}, \{\hat{\mathbf{r}}_j\}) = \sum_j q_j\delta(\mathbf{x} - \hat{\mathbf{r}}_j), \tag{51}$$

where j indexes over all charged particles of charge q_j and position $\hat{\mathbf{r}}_j$ and $\mathbf{x}$ is the global Cartesian coordinate system. This charge density function is used to fix the longitudinal (curl-free) component of the auxiliary polarization field, $\hat{\mathbf{P}}^g(\mathbf{x}, \{\hat{\mathbf{r}}_j\})$, such that

$$\hat{\nabla}\cdot\hat{\mathbf{P}}^g(\mathbf{x}, \{\hat{\mathbf{r}}_j\}) = -\hat{\rho}(\mathbf{x}, \{\hat{\mathbf{r}}_j\}), \tag{52}$$

and the transverse (divergence-free) component must be defined for a given gauge, g. For example, in the Coulomb gauge, $\hat{\mathbf{P}}^{\mathrm{C}}_{\perp} = 0$ and in the multi-polar gauge (the dipole gauge beyond the long-wavelength approximation), $\hat{\mathbf{P}}^{\mathrm{mp}}_{\perp} = \sum_j q_j\hat{\mathbf{r}}_j\int_0^1 ds\,\delta_{\perp}(\mathbf{x} - s\hat{\mathbf{r}}_j)$.

To transform between gauges, a more generalized gauge transformation in terms of the polarization fields is needed

$$\hat{W}_{g\to g'} = \exp\left[\frac{i}{\hbar}\int d\mathbf{x}\,[\hat{\mathbf{P}}^{g'}_{\perp} - \hat{\mathbf{P}}^{g}_{\perp}]\cdot\hat{\boldsymbol{A}}(\mathbf{x})\right], \tag{53}$$

where $\hat{W}_{g\to g'}$ is a unitary operator that transforms an operator from the gauge, g, to the gauge, g', $\hat{\boldsymbol{A}}(\mathbf{x})$ is once again the transverse component of the vector potential, the explicit $\mathbf{x}, \{\hat{\mathbf{r}}_j\}$ dependence is not written for brevity.

With this formalism, the light–matter Hamiltonian in an arbitrary gauge, $\hat{H}_g$, can now be written as

$$\hat{H}_g = \hat{W}_{\mathrm{C}\to g}\hat{H}_{\mathrm{M}}\hat{W}^\dagger_{\mathrm{C}\to g} + \hat{W}_{\mathrm{mp}\to g}\hat{H}_{\mathrm{ph}}\hat{W}^\dagger_{\mathrm{mp}\to g}. \tag{54}$$

Under the long-wavelength approximation, this result reduces to the relations shown in Eqs. (41) and (42). Similar to Sec. II under the long-wavelength approximation, transforming $g \to g'$ follows the simple relation $\hat{H}_{g'} = \hat{W}_{g\to g'}\hat{H}_g\hat{W}_{g\to g'}$.

To resolve gauge ambiguities upon truncation, a similar process to Secs. III C–III E is performed. First, the pure matter and the pure photonic Hamiltonians are projected, $H_{\mathrm{M}} \to \mathcal{H}_{\mathrm{M}}$ and $H_{\mathrm{ph}} \to \mathcal{H}_{\mathrm{ph}}$.

Then, the unitary operator, $\hat{W}_{g\to g'}$ is properly confined in the truncated subspace. For the matter DOFs, the argument in the exponential of $\hat{W}_{g\to g'}$ is no longer given to be linear with $\{\mathbf{r}_j\}$ with the relaxation of the long-wavelength approximation. Due to this, the argument of the exponential cannot be directly projected by $\hat{\mathcal{P}}$. Instead, $\hat{W}_{g\to g'}$ must be represented in terms of $\hat{\mathrm{r}}_j = \hat{\mathcal{P}}\hat{\mathbf{r}}_j\hat{\mathcal{P}}$. In this manner, the polarization field is projected in terms of $\{\hat{\mathrm{r}}_j\}$ such that $\hat{\mathbf{P}}^g(\mathbf{x}, \{\hat{\mathbf{r}}_j\}) \to \hat{\mathcal{P}}^g(\mathbf{x}, \{\hat{\mathrm{r}}_j\})$. For the photonic DOFs, the mode truncation in this regime is done in the same fashion as in Sec. III E, where the vector potential is directly projected as $\hat{\boldsymbol{A}}(\mathbf{x}) \to \hat{\mathcal{P}}\hat{\boldsymbol{A}}(\mathbf{x})\hat{\mathcal{P}} = \hat{\mathcal{A}}(\mathbf{x})$. The gauge transformation in the properly confined in the truncated subspace can then be written as

$$\hat{\mathcal{W}}_{g\to g'} = \exp\left[\frac{i}{\hbar}\int d\mathbf{x}\,[\hat{\boldsymbol{\mathcal{P}}}^{g'}_{\perp} - \hat{\boldsymbol{\mathcal{P}}}^{g}_{\perp}]\cdot\hat{\boldsymbol{\mathcal{A}}}(\mathbf{x})\right], \tag{55}$$

where the $(\mathbf{x}, \{\hat{\mathrm{r}}_j\})$ dependence in $\hat{\mathcal{P}}^g_{\perp}$ is suppressed for brevity.

Finally, the gauge invariant Hamiltonian for an arbitrary gauge, g, can be constructed using the properly confined gauge transformation, $\hat{\mathcal{W}}_{g\to g'}$, as

$$\hat{\mathcal{H}}_g = \hat{\mathcal{W}}_{\mathrm{C}\to g}\hat{\mathcal{H}}_{\mathrm{M}}\hat{\mathcal{W}}^\dagger_{\mathrm{C}\to g} + \hat{\mathcal{W}}_{\mathrm{mp}\to g}\hat{\mathcal{H}}_{\mathrm{ph}}\hat{\mathcal{W}}^\dagger_{\mathrm{mp}\to g}. \tag{56}$$

In this manner, even beyond the long-wavelength approximation, gauge ambiguities can be resolved by carefully representing all operators in terms of truncated coordinate and momentum operators. In Ref. 43, the formal derivation of this method in the context of macroscopic QED is provided at length.

IV. MODEL HAMILTONIANS IN QUANTUM OPTICS

In quantum optics, a two-level atom coupled to a single mode in an optical cavity is a well-studied subject. This leads to well-known model Hamiltonians, such as the Rabi model and the Jaynes–Cummings model. Since these two models are also widely used in recent investigations of polariton chemistry, here we briefly derive them from the PF Hamiltonian.

We consider a molecule with two electronic states

$$\hat{\mathcal{H}}_{\mathrm{M}} = \hat{T} + E_g(R)|g\rangle\langle g| + E_e(R)|e\rangle\langle e|, \tag{57}$$

and the transition dipole is $\boldsymbol{\mu}_{eg} = \langle e|\hat{\boldsymbol{\mu}}|g\rangle$. Note that the permanent dipoles in a molecule $\boldsymbol{\mu}_{ee} = \langle e|\hat{\boldsymbol{\mu}}|e\rangle$, $\boldsymbol{\mu}_{gg} = \langle g|\hat{\boldsymbol{\mu}}|g\rangle$ are not necessarily zero, as opposed to the atomic case where they are always zero. Hence, it is not always a good approximation to drop them.

The Rabi model, however, assumes that one can ignore the permanent dipole moments (PDM) and leads to the dipole operator expression in the subspace $\hat{\mathcal{P}} = |g\rangle\langle g| + |e\rangle\langle e|$ of

$$\hat{\mathcal{P}}\hat{\boldsymbol{\mu}}\hat{\mathcal{P}} = \boldsymbol{\mu}_{eg}(|e\rangle\langle g| + |g\rangle\langle e|) \equiv \boldsymbol{\mu}_{eg}(\hat{\sigma}^\dagger + \hat{\sigma}), \tag{58}$$

where we have defined the creation operator $\hat{\sigma}^\dagger \equiv |e\rangle\langle g|$ and annihilation operator $\hat{\sigma} \equiv |g\rangle\langle e|$ of the electronic excitation. The PF Hamiltonian [Eq. (10)] in the subspace $\hat{\mathcal{P}}$ thus becomes

$$\hat{\mathcal{H}}_{\mathrm{noPDM}} = \hat{\mathcal{H}}_{\mathrm{M}} + \hat{H}_{\mathrm{ph}} + \omega\boldsymbol{A}_0\cdot\boldsymbol{\mu}_{eg}(\hat{\sigma}^\dagger + \hat{\sigma})(\hat{a}^\dagger + \hat{a}) + \omega(\boldsymbol{A}_0\cdot\boldsymbol{\mu}_{eg})^2. \tag{59}$$

Dropping the DSE (the last term) from Eq. (59) leads to the Rabi model

$$\hat{\mathcal{H}}_{\mathrm{Rabi}} = \hat{\mathcal{H}}_{\mathrm{M}} + \hat{H}_{\mathrm{ph}} + \omega\boldsymbol{A}_0\cdot\boldsymbol{\mu}_{eg}(\hat{\sigma}^\dagger + \hat{\sigma})(\hat{a}^\dagger + \hat{a}). \tag{60}$$

13 February 2025 02:07:04

Published under an exclusive license by AIP Publishing

Dropping both the DSE and the counter-rotating terms $\hat{\sigma}^\dagger\hat{a}^\dagger$ and $\hat{\sigma}\hat{a}$ leads to the well-known Jaynes–Cummings (JC) model[103] as follows:

$$\hat{\mathcal{H}}_{\mathrm{JC}} = \hat{\mathcal{H}}_{\mathrm{M}} + \hat{H}_{\mathrm{ph}} + \omega \boldsymbol{A}_0 \cdot \boldsymbol{\mu}_{eg}(\hat{\sigma}^\dagger\hat{a} + \hat{\sigma}\hat{a}^\dagger). \tag{61}$$

This Jaynes–Cummings Hamiltonian is used ubiquitously across the field of quantum optics, from quantum computing[104] applications to fundamental physics experiments.[105,106] For experimentalists and theorists alike, this well-established Hamiltonian is appealing due to its simplicity and intuitive physical interpretation. Equation (61) can be broken down and interpreted in four parts: $\hat{\mathcal{H}}_{\mathrm{M}}$ is the pure matter Hamiltonian, $\hat{H}_{\mathrm{ph}}$ is the pure light Hamiltonian, $\omega \boldsymbol{A}_0 \cdot \boldsymbol{\mu}_{eg}\hat{\sigma}^\dagger\hat{a}$ represents absorption of a photon of energy ω, and $\omega \boldsymbol{A}_0 \cdot \boldsymbol{\mu}_{eg}\hat{\sigma}\hat{a}^\dagger$ represents emission of a photon of energy ω. While in many cases this is a convenient and adequate Hamiltonian for weak coupling strengths, in chemically relevant coupling strengths (strong coupling and beyond), this Jaynes–Cummings Hamiltonian is no longer adequate.

To demonstrate the limitations due to the series of approximations in the Jaynes–Cummings Hamiltonian, we compare it to three other two-level system Hamiltonians to isolate the effect of a given approximation on the accuracy of the polaritonic eigenspectrum. Namely, we will compare it to the Rabi Hamiltonian, the PF Hamiltonian without PDM [Eq. (59)], and introduce a two-level Pauli–Fierz Hamiltonian without DSE,

$$\hat{\mathcal{H}}_{\mathrm{noDSE}} = \hat{\mathcal{H}}_{\mathrm{M}} + \hat{H}_{\mathrm{ph}} + \omega \boldsymbol{A}_0 \cdot \hat{\boldsymbol{\mu}}(\hat{a}^\dagger + \hat{a}). \tag{62}$$

In Fig. 6, $\hat{\mathcal{H}}_{\mathrm{noPDM}}$ and $\hat{\mathcal{H}}_{\mathrm{noDSE}}$ are compared to the Rabi and JC models. This helps explain which approximations lead to the various errors in the JC Hamiltonian eigenspectrum, and provides some insight into why the JC Hamiltonian tends to outperform the Rabi Hamiltonian even though the former has more approximations. Compared to the more rigorous two-level PF Hamiltonian, the JC Hamiltonian makes three additional approximations: the neglection of DSE, the removal of PDM, and the rotating-wave approximation.

As shown in Fig. 6(c), the removal of PDM leads to an increase in the splitting at the various avoided crossings. Then, removing the DSE [in Fig. 6(d)] causes a uniform, R-dependent downward shift for all states. The combination of these approximations gives the Rabi model, as seen in Fig. 6(a). The JC model comes from applying the RWA on the Rabi model. By comparing Figs. 6(a) and 6(b), we see that the RWA cancels some of the errors induced by neglecting the DSE. Due to this partial cancelation of errors, the JC model indeed provides more accurate eigenspectra than the Rabi model in many cases.

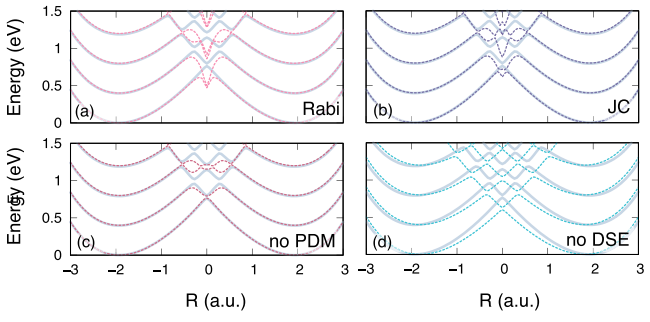

FIG. 6. Comparison of the polariton potential energy surfaces of the Shin–Metiu model coupled to a cavity mode with $A_0 = 0.15$ a.u. and $\omega_c = 400$ meV generated from four different quantum optics model Hamiltonians with the full Pauli–Fierz Hamiltonian plotted in the light gray lines. (a) Rabi Hamiltonian. (b) Jaynes–Cummings (JC) Hamiltonian. (c) Two-level Pauli–Fierz Hamiltonian without the permanent dipole moments (PDM). (d) Pauli–Fierz Hamiltonian without the dipole self-energy (DSE).

V. CONNECTION AND DIFFERENCE WITH THE FLOQUET THEORY

While this review focuses on cavity QED, another popular method for modeling light–matter interactions is the Floquet theory. For the sake of clarity, in this section, we will briefly introduce Floquet theory and contrast it with cavity QED to provide context as to the use cases for each.

We start our analysis by expanding the minimal coupling Hamiltonian in the Coulomb gauge from Eq. (4) for a single electron ($m = 1$) in a potential

$$\hat{H}_{\mathrm{p\cdot A}} = \hat{H}_{\mathrm{M}} - \hat{\boldsymbol{p}} \cdot \hat{\boldsymbol{A}} + \hat{\boldsymbol{A}}^2 + \hat{H}_{\mathrm{ph}}, \tag{63}$$

where in cavity QED, $\hat{\boldsymbol{A}} = \boldsymbol{e}A_0(\hat{a}^\dagger + \hat{a})$ is proportional to the coordinate operator for a quantum harmonic oscillator. Figure 7(b) shows the structure of this Hamiltonian in its matrix formalism.

Typically, Floquet theory is used to describe laser-driven systems, and treats the light field classically (the infinite photon limit). Following the formalism of Ref. 107, $\hat{H}_{\mathrm{ph}}$ is ignored and $\hat{\boldsymbol{A}} \to \boldsymbol{A}(t) = 2A_0\boldsymbol{e}\sin(\omega t)$ is now the classical vector potential for a monochromatic plane wave. The resulting Hamiltonian becomes

$$\hat{H}^{\mathrm{F}}_{\mathrm{p\cdot A}}(t) = \hat{H}_{\mathrm{M}} + A_0^2 - \hbar\nabla \cdot \boldsymbol{e}A_0(e^{i\omega t} - e^{-i\omega t}) + \frac{A_0^2}{2}(e^{2i\omega t} + e^{-2i\omega t}), \tag{64}$$

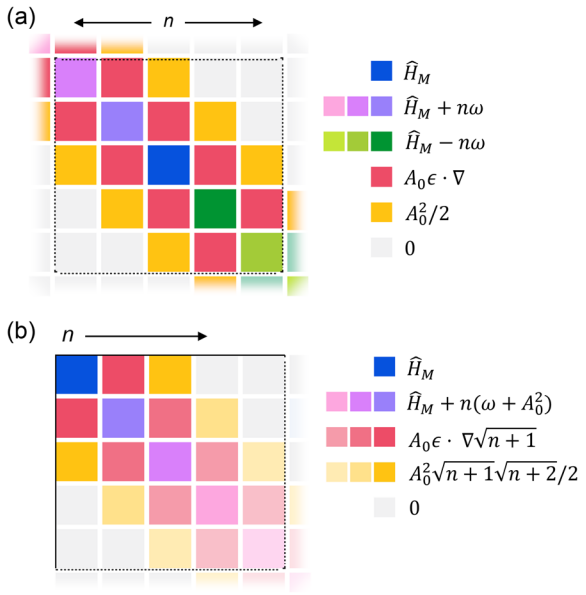

FIG. 7. Comparison with Floquet theory: schematic comparison of the matrix formulation for (a) the time-dependent Schrödinger equation with Floquet theory from Eq. (66) and (b) time-independent Schrödinger equation with the Coulomb gauge Hamiltonian.[107]

13 February 2025 02:07:04

Published under an exclusive license by AIP Publishing

where $\hat{\mathbf{p}} = -i\hbar\nabla$ and the A_0^2 term is just a zero point energy that will be ignored going forward. Since in this perspective light is just a classical, oscillating electromagnetic field with perfect periodicity, a time analog to Bloch's theorem can be used to express a state that satisfies the time-dependent Schrödinger equation, $|\Psi_\alpha(t)\rangle$, in terms of static states, $|\psi_n^\alpha\rangle$ as

$$|\Psi_\alpha(t)\rangle = e^{-iE_\alpha t}\sum_{n=-\infty}^{\infty} e^{in\omega t}|\psi_n^\alpha\rangle, \tag{65}$$

where α indexes over the Floquet states, E_α is a quasienergy, and ω is the driving frequency of the EM field.[108] Using Eqs. (64) and (65), the time-dependent Schrödinger equation in the Sambe space[109] can be written as

$$\begin{aligned} E_\alpha|\Psi_\alpha(t)\rangle = \sum_{n=-\infty}^{\infty}\Big[&\big(\hat{H}_{\mathrm{M}} + n\hbar\omega\big)e^{in\omega t} \\ &+ \hbar\nabla\cdot\mathbf{e}A_0\big(e^{i(n+1)\omega t} - e^{i(n-1)\omega t}\big) \\ &- \frac{A_0^2}{2}\big(e^{i(n+2)\omega t} + e^{i(n-2)\omega t}\big)\Big]|\psi_n^\alpha\rangle. \end{aligned} \tag{66}$$

The right hand side of this equation is an operator whose structure is visualized in Fig. 7(a) with each block corresponding to a given n. The first term of Eq. (66) corresponds to the diagonal blocks, the second term corresponds the light green off diagonal blocks, and the third term corresponds the light blue off diagonal blocks.

It should be noted that this analysis is done in the Coulomb gauge. A similar derivation can be done in the dipole gauge, creating a Floquet equivalent to the PF Hamiltonian shown in Eq. (10). The time-dependent Schrödinger equation can then be written as

$$\begin{aligned} E_\alpha|\Psi_\alpha(t)\rangle = \sum_{n=-\infty}^{\infty}\Big[&\Big(\hat{H}_{\mathrm{M}} + \frac{\hbar}{\omega}(A_0\mathbf{e}\cdot\hat{\boldsymbol{\mu}})^2 + n\hbar\omega\Big)e^{in\omega t} \\ &- A_0\hat{\boldsymbol{\mu}}\cdot\mathbf{e}\big(e^{i(n+1)\omega t} + e^{i(n-1)\omega t}\big)\Big]|\psi_n^\alpha\rangle. \end{aligned} \tag{67}$$

Because there is no $\boldsymbol{A}(t)^2$ term in this Hamiltonian, this Hamiltonian is tridiagonal in the photonic DOF. This significantly decreases the number of n blocks needed to converge the eigenspectrum of this Hamiltonian, making this form more popular for modeling laser-driven systems. A detailed matrix form of the Floquet Hamiltonian can be found in Ref. 110, Chapter 9 (see Fig. 9.5).

Figure 7 shows a schematic comparison of the matrix formulation of the Floquet TDSE matrix (panel a) and the QED Hamiltonian (panel b). In the Floquet TDSE matrix, only the diagonal matrix blocks change with n, and there is no well-defined lower or upper bound for n, since n indexes over temporal unit cells of an infinitely oscillating wave. In contrast, the QED Hamiltonian has n-dependent off diagonal blocks, and n has a lower bound as it is the number of photons. However, in both cases, the general structure of the matrix is similar with the matter Hamiltonian boosted by n on the diagonals and the off diagonal couplings mediated by the p A-type coupling.

Fundamentally, Floquet theory depends on the assumption that the light field is strong enough that the photon number is reaching the infinite limit. In that limit, the matrix structure of Fig. 7(a) converges to that of Fig. 7(b) upon rescaling A_0 and subtracting a zero point energy. As discussed in Ref. 111, the Floquet picture in this limit can be thought of as the QED Hamiltonian when considering a range of Fock states that are sufficiently highly excited such that $\sqrt{n} \approx \sqrt{n+\delta n}$, where δn is the number of Floquet blocks considered. Thus, under this limit of an intense field interacting with the matter, Floquet theory is a natural choice for strongly driven systems since numerical convergence can be reached for a few Floquet blocks. However, in the few photon limit, Floquet theory does break down, and the explicit QED treatment is necessary. It also suggests that the fundamental difference between the Floquet picture and the QED picture arises in the few photon limits. For example, when the hybrid system quickly explores several photon-dressed states $|g, n+1\rangle \rightarrow |e, n\rangle$ through light–matter coupling and $|e, n\rangle \rightarrow |g, n\rangle$ through non-adiabatic coupling $\langle e|\nabla|g\rangle$, the system will explore the different photon number blocks, and the light–matter coupling strength scales with $\sqrt{n}$ due to the operator nature of the coupling term $(\hat{a}^\dagger + \hat{a})$. The Floquet picture, on the other hand, always exhibits the same light–matter coupling strength. This difference between the QED and Floquet pictures has been observed in a recent theoretical study.[112]

VI. GENERALIZED HAMILTONIANS FOR MANY MOLECULES AND MODES

Sections II–V were chiefly concerned with Hamiltonians under the long-wavelength approximation and for a single photonic mode to more clearly demonstrate the relations between different gauges and representations. However, to accurately reproduce the results of experiments such as those with Fabry–Pérot cavities,[9,10,12,113–124] these approximations are no longer adequate. In this manner, we must use generalized Hamiltonians to model such systems, so building on the formalism introduced in Secs. II and III, we use this section as a practical example of creating Hamiltonians that represent more complex systems. In doing so, many modes coupled to many molecules are considered, and we partially relax the long-wavelength approximation such that $\hat{\boldsymbol{A}}$ is no longer spatially invariant while the matter interactions are still approximated as dipoles. Such a Hamiltonian is necessary to describe many molecules coupled to a Fabry–Pérot cavity, as depicted in Fig. 8(a). In that situation, we explicitly consider a 1D array of molecules.[125] Several useful review articles related to this topic can be found in Refs. 126 and 127.

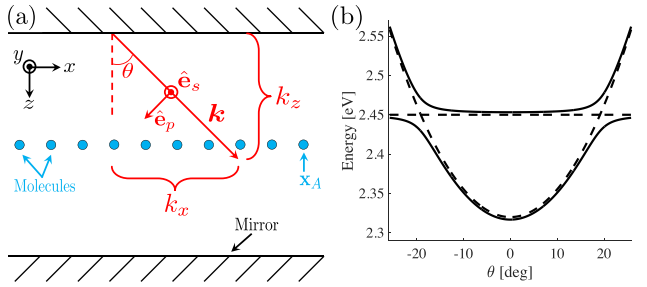

FIG. 8. (a) Schematic of many colinear molecules in a Fabry–Pérot (FP) cavity. $\hat{\mathbf{e}}_s$ and $\hat{\mathbf{e}}_p$ are the unit vectors indicating the directions of the s and p polarized components of $\hat{E}_\perp$, respectively. (b) Schematic dispersion plot of the upper and lower polariton states in a FP cavity (solid lines) as a function of angle (θ) with the same physical parameters as are used in Ref. 113. The dispersion plot of a completely uncoupled system (dashed lines) is also shown to illustrate the Rabi splitting.

13 February 2025 02:07:04

Published under an exclusive license by AIP Publishing

In Fabry–Pérot cavities, the planar mirrors explicitly quantize the vacuum field in the z-direction [see Fig. 8(a)] such that for perfect mirrors, there are only a countable infinite set of allowed k_z wavevectors,

$$k_z = \frac{n_z \pi}{L_z}, \quad n_z = 1, 2, \ldots \infty. \tag{68}$$

Where L_z is the distance between the two mirrors. In the literature,[113,114] k_z is often denoted as $k_\perp$ because it is perpendicular to both mirrors [not to be confused with the transverse component of the field in Eq. (B3a)]. Note that the components of the total wavevector that are parallel to the mirror (k_x and k_y) are not subject to these boundary conditions from the mirrors, and are commonly referred to as $k_\parallel$ in the literature [not to be confused with the longitudinal component of the field, such as Eq. (B2)]. Both k_x and k_y are in principle, quasi-continuous because the boundary length for the lateral directions (x and y in Fig. 8) are generally much larger than the mirror distance L_z. Despite the physical volume of the cavity being very large, strong coupling still occurs experimentally. As such the "cavity quantization volume" is often estimated as $\mathcal{V} = \mathcal{S} \cdot L_z$, where $\mathcal{S}$ is the effective quantization area in which molecules are coupled to the cavity modes.[53] Using the experimentally measured Ω_R and $\mathcal{V}$, one can estimate how many molecules N are effectively coupled to the cavity.[113,128] For example, in Ref 128, they achieve a Rabi splitting of $\Omega_R = 120$ meV and estimate the cavity volume as $\mathcal{V} \sim 1 - 10\mu m^3$, estimating $N \sim 10^7 - 10^8$ molecules effectively coupled to the cavity.

Overall, this leads to many photonic modes that can be energetically close to a matter state transition, such as electronic excitations[113,125,126,129–133] or vibrational excitations.[2,4,10,117,124,134,135] For these cavities, the photonic dispersion relations are the same for both the transverse electric (TE) and transverse magnetic (TM) polarizations, and experimentally, one can easily access both.[133,136,137]

For simplicity, let us focus on the TE mode, and set $k_y = 0$, simplifying the system to a 2D cavity with all modes having the same polarization. For a given mode with the wavevector, $\mathbf{k}$ (see Fig. 8), the total energy of the photon is

$$E_{\rm ph}(\theta) = \hbar\omega_{\boldsymbol{k}} = \frac{\hbar c}{n_{\rm eff}}\sqrt{k_z^2 + k_x^2} = \frac{\hbar c}{n_{\rm eff}} k_z \sqrt{1 + \tan^2\theta}, \tag{69}$$

where c is the speed of the light, $n_{\rm eff}$ is the effective refractive index inside the cavity, and θ is the angle of $\boldsymbol{k}$ from the normal of the mirror [see Fig. 8(a)]. This angle θ is often referred to as the "incident angle" of the photon, which is $\tan\theta = k_x/k_z$. When $\theta = 0$, we have

$$E_{\rm ph}(0) = \frac{\hbar c}{n_{\rm eff}} k_z \equiv \hbar\omega_c, \tag{70}$$

where ω_c is the photon frequency of the fundamental mode of the cavity quantized direction (z-direction), which is commonly used in the single mode approximation of the cavity QED. Further, under the single mode approximation (by setting $k_x = 0$) the photonic momentum $\hbar\mathbf{k}$ (or the field propagation direction) will be perpendicular to the cavity mirror.

In principle, the Fabry–Pérot cavity has a countable infinite set of possible k_z that satisfy the mirror boundary conditions [Eq. (68)]. Often, one only considers the single k_z that is close to the matter excitation energy. However, when $E_{\rm ph}(0)$ is much smaller than the matter excitation energy, multiple modes that contain various k_z [Eq. (68)] in the range of matter-energy and a given range of θ have to be considered.[129,132] In this review, we only consider the case for a single k_z (such that $k_z = \pi/L_z$).

Note that for Fabry–Pérot cavities, $\omega_{\boldsymbol{k}}$ is polarization independent, so typically only the TE mode is considered, as is the case of this example. We emphasize that for a *plasmonic* cavity, Eq. (69) no longer always holds. For example, the plasmonic cavities in Ref. 138 and 139 have a similar dispersion relation for the TM polarization $\omega_{\boldsymbol{k},\rm TM} = \frac{c}{n_{\rm eff}}\sqrt{k_x^2 + \left(\frac{2\pi}{a_x}\right)^2}$, but a linear dispersion for the TE mode $\omega_{\boldsymbol{k},\rm TE} = \frac{c}{n_{\rm eff}}\left(\frac{2\pi}{a_x} \pm k_x\right)$, where a_x is the lattice constant in the x-direction for the plasmonic lattice and $n_{\rm eff}$ is the effective index of refraction of the ambient material in the cavity. In such cases where the cavity dispersion is polarization dependent, both the TE and TM polarizations must be explicitly considered.[138–143] However, for the purpose of this case study, we will simply look at the TE polarization in a Fabry–Pérot cavity. We refer the reader to Ref. 140 for further discussions on plasmonic cavities.

With the motivation of this model in mind, we use this section as a case study on formulating generalized Hamiltonians that are computationally accessible, starting from the fundamental $\mathbf{p} \cdot \mathbf{A}$ Hamiltonian. We first take this into a generalized dipole-gauge Hamiltonian and then further approximate and simplify it to a generalized Tavis–Cummings Hamiltonian.

A. Generalized dipole-gauge Hamiltonian

When considering many molecules in a line coupled to the many modes in a Fabry–Pérot cavity [such as in Fig. 8(a)], often any inter-mode coupling between different k_x-modes such as phononic coupling is ignored. As such the eigenspectrum of such a system is plotted on a dispersion plot [see Fig. 8(b)], where for each point along the k_x (or equivalently θ) axis, the Hamiltonian is projected to the set of modes with the said k_x and diagonalized. This truncation is classified by the projection operator,

$$\hat{\mathcal{P}}_{k_x} = \hat{\mathbb{1}}_{\rm M} \otimes \sum_{k_z, n_{k_x,k_z}} |n_{k_x,k_z}\rangle\langle n_{k_x,k_z}|, \tag{71}$$

where $\hat{\mathbb{1}}_{\rm M}$ is the identity for all matter degrees of freedom, and $\{|n_{k_x,k_z}\rangle\}$ are the Fock states for a given k_x and k_z. To avoid gauge ambiguities, this mode truncation can be performed as discussed in Ref. 102, where the $\hat{\mathcal{P}}_{k_x}$ enters the exponential of the PZW operator [see Eq. (44)]. Then, for each k_x, this truncated Hamiltonian is diagonalized to find the dispersion plots [see Fig. 8(b)] and corresponding Hopfield[144] coefficients as a function of k_x.

To perform these calculations in the dipole gauge, which is advantageous for molecular systems, we start from the minimal coupling Hamiltonian [Eq. (4)], and group the matter system into well-separated molecules (i.e., where the electronic wavefunctions have negligible intermolecular overlap).[145] This will allow us to perform a "multi-centered" PZW transformation to form a generalized dipole gauge Hamiltonian for this system.

In such circumstances (when the intermolecular distances are much longer than the intramolecular distances), we can write $\hat{A}(\hat{\mathbf{x}}_j) \approx \hat{A}(\bar{\mathbf{x}}_A)$ for all particles, j, within the molecule, A, with the center of mass, $\bar{\mathbf{x}}_A$. This is a much less restrictive form of the long-wavelength approximation, where now we are just approximating that the field is

13 February 2025 02:07:04

Published under an exclusive license by AIP Publishing

slowly varying across a given molecule, not the entire system. The total Hamiltonian is then written as

$$\hat{H}^{[N]}_{\text{p·A}} = \sum_{\boldsymbol{k}} \hbar\omega_{\boldsymbol{k}} \hat{a}^\dagger_{\boldsymbol{k}} \hat{a}_{\boldsymbol{k}} + \sum_{A,j\in A} \frac{1}{2m_j} (\hat{\boldsymbol{p}}_j - z_j \hat{\boldsymbol{A}}(\bar{\mathbf{x}}_A))^2 + \hat{V}^{AA}_{\text{coul}} + \sum_{A\neq B} \hat{V}^{AB}_{\text{coul}}, \tag{72}$$

where $\{A, B\}$ index over the molecules in the system whose centers of mass are located at $\bar{\mathbf{x}}_A$, $\{j\}$ indexes over each charged particle j in the molecule A, $\hat{V}^{AA}_{\text{coul}}$ is the intramolecular Coulomb potential in molecule A, and $\hat{V}^{AB}_{\text{coul}}$ is the intermolecular Coulomb potential between molecules A and B.

Now to transform this into the dipole gauge, we use the PZW operator [Eq. (5)], but now with $\hat{\boldsymbol{A}}(\bar{\mathbf{x}}_A)$ spatially varying inside the cavity (but still approximated as constant within a given molecule)

$$\hat{\boldsymbol{A}}(\bar{\mathbf{x}}_A) = \sum_{\boldsymbol{k},n} \sqrt{\frac{\hbar}{2\epsilon_0\omega_{\boldsymbol{k}}\mathcal{V}}} \hat{\boldsymbol{e}}_n [e^{-i\boldsymbol{k}\cdot\bar{\mathbf{x}}_A} \hat{a}^\dagger_{\boldsymbol{k},n} + e^{i\boldsymbol{k}\cdot\bar{\mathbf{x}}_A} \hat{a}_{\boldsymbol{k},n}] \tag{73}$$

where the general expression of the quantized electric field $E_\perp$ and magnetic field $\hat{B}$ can be found in standard QED textbooks (e.g., Refs. 42 and 145 or the Appendix of Ref. 19) or in Appendix B.

The corresponding PZW gauge transform operator becomes a *multi-centered* PZW operator[145,146] expressed as

$$\hat{U}_N = \exp\left[-\frac{i}{\hbar}\sum_{A=1}^{N} \hat{\boldsymbol{\mu}}_A \cdot \hat{\boldsymbol{A}}(\bar{\mathbf{x}}_A)\right], \tag{74}$$

which has specific centers of molecules $\bar{\mathbf{x}}_A$. This $\hat{U}_N$ is still a boost operator on $\hat{\boldsymbol{p}}_j$, since we are still assuming that the individual molecules can be well described by their dipoles, so $\hat{U}_N \hat{\boldsymbol{p}}_j \hat{U}^\dagger_N \approx \hat{\boldsymbol{p}}_j + q_j \hat{\boldsymbol{A}}(\bar{\mathbf{x}}_A)$. We can also evaluate $\hat{U}_N \hat{a}_{\boldsymbol{k}} \hat{U}^\dagger_N$ as

$$\hat{U}_N \hat{a}_{\boldsymbol{k}} \hat{U}^\dagger_N = \hat{a}_{\boldsymbol{k}} + \sum_A i\sqrt{\frac{\hbar}{2\epsilon_0\omega_{\boldsymbol{k}}\mathcal{V}}} \hat{\boldsymbol{e}}_n \hat{\boldsymbol{\mu}}_A(\hat{\boldsymbol{R}}_A) e^{-i\boldsymbol{k}\cdot\hat{\mathbf{x}}_A}, \tag{75}$$

where $\hat{\boldsymbol{\mu}}_A(\hat{\boldsymbol{R}}_A)$ is the dipole operator of molecule A with the nuclear configuration $\hat{\boldsymbol{R}}_A$.

Additionally, the phase rotation from Eq. (9) can be generalized for many modes as

$$\hat{U}^{[N]}_\phi = e^{-i\frac{\pi}{2}\sum_{\mathbf{k},n} \hat{a}^\dagger_{\mathbf{k},n}\hat{a}_{\mathbf{k},n}}, \tag{76}$$

where all the modes now experience a phase rotation.

Now, we can write our generalized dipole gauge Hamiltonian in full space as

$$\begin{aligned}\hat{H}^{[N]}_{\text{d·E}} &= \hat{U}^{[N]}_\phi \hat{U}_N \hat{H}^{[N]}_{\text{p·A}} \hat{U}^\dagger_N \hat{U}^{[N]\dagger}_\phi \\ &= \hat{H}_{\text{M}} + \sum_{\mathbf{k},n}\Bigg[\hbar\omega_{\mathbf{k}}\left(\hat{a}^\dagger_{\mathbf{k}}\hat{a}_{\mathbf{k}} + \frac{1}{2}\right) \\ &\quad + \sum_A \Bigg(\sqrt{\frac{\omega_{\mathbf{k}}}{2}}\boldsymbol{\lambda}_{\mathbf{k},n}\cdot\hat{\boldsymbol{\mu}}_A(\mathbf{R}_A)(\hat{a}_{\mathbf{k}}e^{i\mathbf{k}\cdot\mathbf{x}_A} + \hat{a}^\dagger_{\mathbf{k}}e^{-i\mathbf{k}\cdot\mathbf{x}_A}) \\ &\quad + \sum_B \frac{1}{2}(\boldsymbol{\lambda}_{\mathbf{k},n}\cdot\hat{\boldsymbol{\mu}}_A(\mathbf{R}_A))(\boldsymbol{\lambda}_{\mathbf{k},n}\cdot\hat{\boldsymbol{\mu}}_B(\mathbf{R}_B))e^{-i\mathbf{k}\cdot(\mathbf{x}_A-\mathbf{x}_B)}\Bigg)\Bigg],\end{aligned} \tag{77}$$

where we introduced a coupling parameter for this more complicated system, $\boldsymbol{\lambda}_{\boldsymbol{k},n} = \sqrt{\frac{1}{\epsilon_0\mathcal{V}}}\hat{\boldsymbol{e}}_{\boldsymbol{k},n}$. While this form is significantly more manageable to calculate compared to the fundamental minimal coupling Hamiltonian, it still suffers from very unfavorable scaling in its basis size. For j molecules with l states and mk_z-modes with n Fock states, the basis size is $l^j n^m$, which is nearly impossible for all but the simplest model matter systems. To remedy this, we need to make some further approximations to the many-mode, many-molecule equivalent of the Jaynes–Cummings model, the so-called generalized Tavis–Cummings model.

B. Generalized Tavis–Cummings Hamiltonian

Intuitively, the generalized Tavis–Cummings (GTC) Hamiltonian is to the generalized dipole gauge Hamiltonian [Eq. (77)] as the Jaynes–Cummings Hamiltonian [Eq. (61)] is to the traditional dipole gauge Hamiltonian [Eq. (7)]. In this manner, there are a series of approximations from Eq. (77) to obtain the GTC Hamiltonian. Namely, we first truncate each molecule to the two-level approximation and remove permanent dipole, such that the dipole operator for a given molecule can be written as $\hat{\boldsymbol{\mu}}_A = \boldsymbol{\mu}^{\text{eg}}_A \hat{\sigma}_x$, where $\boldsymbol{\mu}^{\text{eg}}_A$ is the transition dipole moment between the ground and excited states for the molecule A. Then, the dipole self-energy terms [last line of Eq. (77)] are entirely neglected. Finally, the rotating wave approximation is performed such that for the interaction terms become

$$\begin{aligned}&\sqrt{\frac{\omega_{\mathbf{k}}}{2}}\boldsymbol{\lambda}_{\boldsymbol{k},n}\cdot\hat{\boldsymbol{\mu}}_A(\mathbf{R}_A)(\hat{a}_{\boldsymbol{k}}e^{i\mathbf{k}\cdot\mathbf{x}_A} + \hat{a}^\dagger_{\boldsymbol{k}}e^{-i\mathbf{k}\cdot\mathbf{x}_A}) \\ &\quad\rightarrow \sqrt{\frac{\omega_{\mathbf{k}}}{2}}\boldsymbol{\lambda}_{\boldsymbol{k},n}\cdot\boldsymbol{\mu}^{\text{eg}}_A(\mathbf{R}_A)(\hat{\sigma}^\dagger_A\hat{a}_{\boldsymbol{k}}e^{i\mathbf{k}\cdot\mathbf{x}_A} + \hat{\sigma}_A\hat{a}^\dagger_{\boldsymbol{k}}e^{-i\mathbf{k}\cdot\mathbf{x}_A}),\end{aligned} \tag{78}$$

where $\hat{\sigma}_A$ is the lowering operator for molecule A's two-level system. This series then leads to an expression of the GTC Hamiltonian,

$$\begin{aligned}\hat{H}_{\text{GTC}} = \hat{H}_{\text{M}} + \sum_{\boldsymbol{k},n}\Bigg[&\hbar\omega_{\boldsymbol{k}}\left(\hat{a}^\dagger_{\boldsymbol{k}}\hat{a}_{\boldsymbol{k}} + \frac{1}{2}\right) \\ &+ \sqrt{\frac{\omega_{\mathbf{k}}}{2}}\boldsymbol{\lambda}_{\boldsymbol{k},n}\cdot\boldsymbol{\mu}^{\text{eg}}_A(\hat{\sigma}^\dagger_A\hat{a}_{\boldsymbol{k}}e^{i\mathbf{k}\cdot\mathbf{x}_A} + \hat{\sigma}_A\hat{a}^\dagger_{\boldsymbol{k}}e^{-i\mathbf{k}\cdot\mathbf{x}_A})\Bigg].\end{aligned} \tag{79}$$

This generalized Tavis–Cummings model now lives only in the single-excitation subspace, reducing the basis size to $j + m + 1$ for j molecules and mk_z-modes. This drastically reduces the computational cost of modeling large systems. Recently, studies involving this GTC Hamiltonian have been able to shine new light on the experimentally found dispersion plots,[113,114,147,148] [see Fig. 8(b)].

One such observed phenomenon that can be predicted by the GTC is the presence of collective "bright" and "dark" states (referring to the presence (or lack thereof) of photonic character) formed by the hybridization of each molecule with each k_x mode. These states, schematically illustrated in the dispersion plot in Fig. 8(b) are the result of the light–matter hybridization of j singly-excited molecular states hybridizing with a single photon. These $j + 1$ excited states exactly become two bright states and $j - 1$ dark states, where the bright states are the many molecule equivalents of the JC $|\pm\rangle$ states [see the solid lines in Fig. 8(b)]. The dark states, however, have no photonic character and are the linear combinations of the matter such that these

13 February 2025 02:07:04

Published under an exclusive license by AIP Publishing

collective states have no transition dipole and are completely decoupled from the polaritonic "bright" states [see the flat dashed line in Fig. 8(b)].

VII. CONCLUSIONS AND OUTLOOK

There has been a great deal of progress in the last few years in understanding different representations and gauges to model these cQED systems. In an effort to summarize the many different approaches to this problem in one place, this review focuses on the various ways to formulate cQED Hamiltonians for different levels of approximation and applications.

Section II discusses three different representations to express the cavity–matter hybrid system in full space. It begins with the minimal coupling Hamiltonian in the Coulomb gauge (Sec. II A), where the light–matter interaction is mediated through the matter momentum and the photonic field's vector potential. Then, the Power-Zienau-Woolly (PZW) transformation is introduced under the long-wavelength approximation (or equivalently dipole approximation), and the dipole gauge and Pauli–Fierz Hamiltonians (Sec. II B) are derived from the minimal coupling Hamiltonian. Finally, a new representation, called the asymptotically decoupled Hamiltonian, is presented from the minimal coupling Hamiltonian and its advantageous convergence properties are discussed (Sec. II C).

In Sec. III, we go on to discuss complications that ensue due to a finite truncation of the infinite Hilbert space Hamiltonians in Sec. II and their corresponding resolutions. When projecting the dipole gauge Hamiltonian (Sec. II B) and minimal coupling Hamiltonian (Sec. II A) to a finite matter eigenbasis, the polariton energies do not match, indicating that performing a simple projection breaks the gauge invariance (Sec. III B). These gauge ambiguities can be understood since projecting the PZW operator loses its unitary property. By properly truncating all operators, these ambiguities can be resolved a so-called properly truncated Coulomb gauge Hamiltonian is formed (Sec. III C). Building off of this, by performing a change of basis and a phase rotation, the polarized Fock state representation can be formed from this properly truncated Coulomb gauge Hamiltonian, which for molecular systems can have its eigenspectrum converge for a very small basis set (Sec. III D). It has also been shown that truncating the number of photonic modes also leads to gauge ambiguities that can be resolved using a method similar to the resolution for the matter DOFs (Sec. III E). Additionally, these gauge ambiguities have recently been resolved for Hamiltonians beyond the long-wavelength approximation (Sec. III F).

Section IV then connects the rigorous cQED Hamiltonians from Secs. II and III to the more commonly used quantum optic models such as the Jaynes–Cummings model and the Rabi model. This section, carefully discusses the different levels of approximations that each model are under and compares the accuracy of each model.

Additionally, Sec. V contrasts the cQED methods discussed in this review with the commonly used Floquet theory for laser driven media. This shows the limits in which the cQED methods approach the Floquet picture, as well as the reasons to use one method over another.

Since many experiments are done in Fabry–Pérot cavities, Sec. VI discusses the Hamiltonians used for such systems. Since Fabry–Pérot cavities are made of flat mirrors, they have a quasi-continuous spectrum of photonic modes and typically hold many molecules, so it is helpful to use Hamiltonians that explicitly consider this. This section discusses the generalized multi-center dipole gauge Hamiltonian that considers many molecules as individual dipoles inside a cavity (Sec. VI A). Then, by making a series of approximations, the generalized Tavis–Cummings Hamiltonian is formulated, which can drastically reduce the computational cost of modeling these very complex systems (Sec. VI B).

Even with the numerous recent advances in the field, there are still many mysteries to be solved in polariton chemistry. Typically, the first step in approaching these challenges is to formulate the Hamiltonian to describe the system. With a summary of the different representations, truncation schemes, and levels of approximation in various cQED Hamiltonians, we hope that this review will provide theorists with a full toolbox such that they can fit the best method to their own application and start unraveling the mysteries of the field.

ACKNOWLEDGMENTS

This work was supported by the Air Force Office of Scientific Research (Grant No. FA9550-23-1-0438), as well as by the National Science Foundation Award (Grant No. CHE-2244683). M. T. appreciates the support from the National Science Foundation Graduate Research Fellowship Program under Grant No. DGE-1939268. P. H. appreciates the support of the Cottrell Scholar Award (a program by the Research Corporation for Science Advancement). Computing resources were provided by the Center for Integrated Research Computing (CIRC) at the University of Rochester. The authors want to acknowledge enlightening discussions with Angel Rubio, Abraham Nitzan, Neepa Maitra, Adam Stokes, Ahsan Nazir, Peter Milonni, Sarada Rajeev, Tao Li, Michael Ruggenthaler, and David Reichman.

AUTHOR DECLARATIONS

Conflict of Interest

The authors have no conflicts to disclose.

Author Contributions

Michael A. D. Taylor: Conceptualization (equal); Formal analysis (lead); Investigation (equal); Methodology (equal); Project administration (equal); Software (lead); Validation (equal); Visualization (equal); Writing – original draft (lead); Writing – review & editing (equal). **Arkajit Mandal:** Conceptualization (equal); Data curation (equal); Formal analysis (equal); Investigation (equal); Methodology (equal); Project administration (equal); Software (equal); Supervision (equal); Validation (equal); Visualization (equal); Writing – original draft (equal); Writing – review & editing (supporting). **Pengfei Huo:** Conceptualization (equal); Formal analysis (equal); Funding acquisition (equal); Investigation (equal); Project administration (equal); Resources (equal); Supervision (equal); Writing – original draft (equal); Writing – review & editing (equal).

DATA AVAILABILITY

The data that support the findings of this work are available from the corresponding author under reasonable request.

APPENDIX A: REVIEW OF MOLECULAR HAMILTONIANS

Here, we briefly review some basic knowledge of the molecular Hamiltonian, which will be useful for our discussions of molecular

13 February 2025 02:07:04

Published under an exclusive license by AIP Publishing

cavity QED. We begin by defining the matter Hamiltonian as follows:

$$\hat{H}_{\mathrm{M}} = \hat{\mathbf{T}} + \hat{V}(\hat{\mathbf{x}}) = \sum_j \frac{1}{2m_j}\hat{\mathbf{p}}_j^2 + \hat{V}(\hat{\mathbf{x}}_j), \tag{A1}$$

where j is the index of the jth charged particle (including all electrons and nuclei), with the corresponding mass, m_j, and *canonical* momentum, $\hat{\mathbf{p}}_j = -i\hbar\nabla_j$. We denote electronic coordinate with $\hat{\mathbf{r}}$, and nuclear coordinate with $\hat{\mathbf{R}}$, and use $\hat{\mathbf{x}}_j \in \{\mathbf{r}_j, \mathbf{R}_j\}$ to represent either the electron or nucleus, with $\hat{\mathbf{x}}$ being the coordinate operator for all charged particles. Further, $\hat{\mathbf{T}} = \hat{\mathbf{T}}_{\mathbf{R}} + \hat{\mathbf{T}}_{\mathbf{r}}$ is the kinetic energy operator for all charged particles, where $\hat{\mathbf{T}}_{\mathbf{R}}$ and $\hat{\mathbf{T}}_{\mathbf{r}}$ represent the kinetic energy operator for nuclei and for electrons, respectively. Further, $\hat{V}(\hat{\mathbf{x}})$ is the potential operator that describes the Coulombic interactions among the electrons and nuclei. The electronic Hamiltonian is often defined as

$$\hat{H}_{\mathrm{el}} = \hat{H}_{\mathrm{M}} - \hat{\mathbf{T}}_{\mathbf{R}} = \hat{\mathbf{T}}_r + \hat{V}(\hat{\mathbf{x}}), \tag{A2}$$

which includes the kinetic energy of electrons, electron–electron interactions, electron–nuclear interactions, and nuclear–nuclear interactions. The essential task of the electronic structure community is focused on solving the eigenstates of $\hat{H}_{\mathrm{el}}$ at a particular nuclear configuration $\mathbf{R}$ as follows:

$$\hat{H}_{\mathrm{el}}|\psi_\alpha(\mathbf{R})\rangle = E_\alpha(\mathbf{R})|\psi_\alpha(\mathbf{R})\rangle, \tag{A3}$$

where $E_\alpha(\mathbf{R})$ is commonly referred to as the α_{th} potential energy surface (PES) or adiabatic energy, and $|\psi_\alpha(\mathbf{R})\rangle$ is commonly referred to as the α_{th} adiabatic electronic state.

In the adiabatic electronic basis $\{|\psi_\alpha(\mathbf{R})\rangle\}$, the matter Hamiltonian can be expressed as[70,72]

$$\hat{H}_{\mathrm{M}} = \frac{1}{2\mathbf{M}}\left(\hat{\mathbf{P}} - i\hbar\sum_{\alpha\beta}\mathbf{d}_{\alpha\beta}|\psi_\alpha\rangle\langle\psi_\beta|\right)^2 + \sum_\alpha E_\alpha(\mathbf{R})|\psi_\alpha\rangle\langle\psi_\alpha|, \tag{A4}$$

where $\hat{\mathbf{P}}$ is the nuclear momentum operator, $\mathbf{M}$ is the tensor of nuclear masses, and we have used the shorthand notation $|\psi_\alpha\rangle \equiv |\psi_\alpha(\mathbf{R})\rangle$, and $\mathbf{d}_{\alpha\beta}$ is the derivative coupling expressed as

$$\mathbf{d}_\alpha = \langle\psi_\alpha(\mathbf{R})|\nabla_{\mathbf{R}}|\psi_\alpha(\mathbf{R})\rangle. \tag{A5}$$

Note that the above equation is equivalent[70,72] to the commonly used form of the vibronic Hamiltonian

$$\hat{H}_{\mathrm{M}} = -\frac{\hbar^2}{2\mathbf{M}}\sum_{\alpha\beta}\left[\nabla_{\mathbf{R}}^2\delta_{\alpha\beta} + 2\mathbf{d}_{\alpha\beta}\cdot\nabla_{\mathbf{R}} + D_{\alpha\beta}\right]|\psi_\alpha\rangle\langle\psi_\beta| + \sum_\alpha E_\alpha(\mathbf{R})|\psi_\alpha\rangle\langle\psi_\alpha|,$$

where $D_{\alpha\beta} = \langle\psi_\alpha(\mathbf{R})|\nabla_R^2|\psi_\beta(\mathbf{R})\rangle$ is the second derivative coupling. A simple proof can be found in Ref. 18.

Later, we will see that the dipole operator plays an important role in describing light–matter interactions, so let us spend a bit of time to discuss the molecular dipole operator. The total dipole operator of the entire molecule is

$$\hat{\boldsymbol{\mu}} = \sum_j z_j\hat{\mathbf{x}}_j, \tag{A6}$$

where z_j is the charge for the jth charged particle. The matrix elements of the total dipole operators can be obtained using the adiabatic states as

$$\boldsymbol{\mu}_{\alpha\beta}(\mathbf{R}) = \langle\psi_\alpha(\mathbf{R})|\hat{\boldsymbol{\mu}}|\psi_\beta(\mathbf{R})\rangle. \tag{A7}$$

For $\alpha \neq \beta$, $\boldsymbol{\mu}_{\alpha\beta}(\mathbf{R})$ is referred to as the transition dipole between state $|\psi_\alpha\rangle$ and $|\psi_\beta\rangle$, while $\boldsymbol{\mu}_{\alpha\alpha}(\mathbf{R})$ is commonly referred to as the permanent dipole for state $|\psi_\alpha\rangle$.

It is often difficult to get accurate electronic states for highly excited adiabatic states. It is thus ideal to consider a Hilbert subspace of the electronic Hamiltonian. Considering a finite subset of electronic states $\{|\psi_\alpha\rangle\}$ [see Eq. (A3)] where there is a total of $\mathcal{N}$ matter states, one can define the following projection operator:

$$\hat{\mathcal{P}} = \sum_{\alpha=1}^{\mathcal{N}}|\psi_\alpha(\mathbf{R})\rangle\langle\psi_\alpha(\mathbf{R})|, \tag{A8}$$

which defines the truncation of the full electronic Hilbert space $\hat{\mathbb{1}}_{\mathrm{r}} = \hat{\mathcal{P}} + \hat{\mathcal{Q}}$ which has an infinite basis, to a subspace $\hat{\mathcal{P}}$ that contains a total of $\mathcal{N}$ states, where $\hat{\mathbb{1}}_{\mathrm{r}}$ is the identity operator in the electronic Hilbert subspace (the subspace containing all of the electron DOF) and $\hat{\mathcal{Q}} = \hat{\mathbb{1}}_{\mathrm{r}} - \hat{\mathcal{P}}$ is the subspace being projected out.

Using the projection operator, one can define the projected matter Hamiltonian (or the truncated matter Hamiltonian) as follows:

$$\hat{\mathcal{H}}_{\mathrm{M}} = \hat{\mathcal{P}}\hat{H}_{\mathrm{M}}\hat{\mathcal{P}} = \hat{\mathcal{P}}\hat{\mathbf{T}}\hat{\mathcal{P}} + \hat{\mathcal{P}}\hat{V}(\hat{\mathbf{x}})\hat{\mathcal{P}}. \tag{A9}$$

Throughout this review, we use calligraphic symbols (such as $\hat{\mathcal{H}}_{\mathrm{M}}$) to indicate operators in the truncated Hilbert space.

One can also explicitly write the dipole operator in the truncated Hilbert space as follows:

$$\hat{\mathcal{P}}\hat{\boldsymbol{\mu}}\hat{\mathcal{P}} = \sum_{\alpha=1}^{\mathcal{N}}\boldsymbol{\mu}_{\alpha\alpha}(\mathbf{R})\,|\psi_\alpha(\mathbf{R})\rangle\langle\psi_\alpha(\mathbf{R})| + \sum_{\alpha\neq\beta}\boldsymbol{\mu}_{\alpha\beta}(\mathbf{R})\,|\psi_\alpha(\mathbf{R})\rangle\langle\psi_\beta(\mathbf{R})|. \tag{A10}$$

In the *same* truncated electronic subspace as defined by $\hat{\mathcal{P}}$ [Eq. (A8)], we can diagonalize the dipole matrix in Eq. (A10) to obtain

$$\hat{\mathcal{P}}\hat{\boldsymbol{\mu}}\hat{\mathcal{P}} = \sum_{\nu}^{\mathcal{N}}\boldsymbol{\mu}_{\nu\nu}(\mathbf{R})\,|\phi_\nu\rangle\langle\phi_\nu|, \tag{A11}$$

where $|\phi_\nu\rangle$ is the eigenstate of the projected dipole operator $\hat{\mathcal{P}}\hat{\boldsymbol{\mu}}\hat{\mathcal{P}}$ with

$$|\phi_\nu\rangle = \sum_\alpha^{\mathcal{N}} c_\alpha^\nu(\mathbf{R})|\psi_\alpha(\mathbf{R})\rangle, \tag{A12}$$

and $c_\alpha^\nu(\mathbf{R}) = \langle\psi_\alpha(\mathbf{R})|\phi_\nu\rangle$.

The projection operator in Eq. (A8) can also be expressed as

$$\hat{\mathcal{P}} = \sum_{\nu=1}^{\mathcal{N}}|\phi_\nu\rangle\langle\phi_\nu|, \tag{A13}$$

which is simply a unitary transform of Eq. (A8) [from the $|\psi_\alpha(\mathbf{R})\rangle$-representation to the $|\phi_\nu\rangle$-representation].

13 February 2025 02:07:04

Published under an exclusive license by AIP Publishing

In the literature, the eigenstates of $\hat{\mathcal{P}}\hat{\boldsymbol{\mu}}\hat{\mathcal{P}}$, $\{|\phi_\nu\rangle\}$, are referred to as the Mulliken–Hush (MH) diabatic states,[68,73,149–151] which are commonly used as approximate *diabatic* states that are defined based on their characters. They are approximate diabatic states in the sense that

$$\langle\phi_\nu|\nabla_{\mathbf{R}}|\phi_\epsilon\rangle \approx 0, \tag{A14}$$

hence, we drop the $\mathbf{R}$-dependence in $|\phi_\nu\rangle$. Constructing rigorous diabatic states (where the derivative coupling is rigorously zero for all possible nuclear configurations) in a finite set of electronic Hilbert spaces is generally impossible, except for diatomic molecules. Recent theoretical progress on diabatization can be found in Refs. 71, 152 and 153.

In the electronic subspace defined within the MH diabatic subspace using $\hat{\mathcal{P}}$ [Eq. (A13)], $\hat{H}_{\rm el}$ [Eq. (A2)] has off diagonal (or "diabatic") coupling terms

$$V_{\nu\epsilon}(\mathbf{R}) = \langle\phi_\nu|\hat{H}_{\rm el}|\phi_\epsilon\rangle = \sum_\alpha c_\alpha^{\nu*}(\mathbf{R})c_\alpha^{\epsilon}(\mathbf{R})\langle\psi_\alpha|\hat{H}_{\rm el}|\psi_\alpha\rangle. \tag{A15}$$

We can explicitly express the matter state projected

$$\hat{\mathcal{H}}_{\rm M} = \hat{T}_{\mathbf{R}} + \sum_\nu V_{\nu\nu}(\mathbf{R})\,|\psi_\nu\rangle\langle\psi_\nu| + \sum_{\nu\neq\epsilon} V_{\nu\epsilon}(\mathbf{R})\,|\psi_\nu\rangle\langle\psi_\epsilon|. \tag{A16}$$

This is also the molecular Hamiltonian for any diabatic representation.

APPENDIX B: REVIEW OF QUANTUM ELECTRODYNAMICS

We provide a quick review of quantum electrodynamics (QED).[17,21] We begin by writing the electric field as $\hat{\mathbf{E}}(\mathbf{r}) = \hat{\mathbf{E}}_\parallel(\mathbf{r}) + \hat{\mathbf{E}}_\perp(\mathbf{r})$, with its longitudinal part $\hat{\mathbf{E}}_\parallel(\mathbf{r})$ that is curl-free (irrotational), $\nabla\times\hat{\mathbf{E}}_\parallel(\mathbf{r}) = 0$, and the transverse part, $\hat{\mathbf{E}}_\perp(\mathbf{r})$, that is divergence-free (solenoidal), $\nabla\cdot\hat{\mathbf{E}}_\perp(\mathbf{r}) = 0$. The magnetic field is purely transverse $\hat{\mathbf{B}}(\mathbf{r}) = \hat{\mathbf{B}}_\perp(\mathbf{r})$, because it is divergence-free $\nabla\cdot\hat{\mathbf{B}}(\mathbf{r}) = 0$. These fields have spatial dependence, with spatial coordinate $\mathbf{r}$ (not to be confused with the electronic coordinate operator, $\hat{\mathbf{r}}$).

In the context of cavity QED, most simulations are performed in one of two gauges, either the Coulomb gauge[42] or the dipole gauge,[154–156] where the term "gauge" refers to the specific representation of the vector potential $\hat{\boldsymbol{A}}$. Expressing $\hat{\boldsymbol{A}} = \hat{\boldsymbol{A}}_\parallel + \hat{\boldsymbol{A}}_\perp$, with its longitudinal part $\hat{\boldsymbol{A}}_\parallel$ that is curl-free $\nabla\times\hat{\boldsymbol{A}}_\parallel = 0$, and the transverse part $\hat{\boldsymbol{A}}_\perp$ that is divergence-free $\nabla\cdot\boldsymbol{A}_\perp = 0$. In principle, one can do gauge transformations that change the longitudinal part $\hat{\boldsymbol{A}}_\parallel$, because the physically observed quantities will not change (e.g., the magnetic field, since $\hat{\mathbf{B}} = \nabla\times\hat{\boldsymbol{A}} = \nabla\times\hat{\boldsymbol{A}}_\perp$). One often refers to fixing a gauge by choosing the value of $\nabla\times\hat{\boldsymbol{A}}$ such that the gauge transformation is effectively adding an additional $\nabla\chi$ component to $\hat{\boldsymbol{A}}_\parallel$, which is purely longitudinal because when χ is a scalar function in space, $\nabla\chi$ is curl-free ($\nabla\times\nabla\chi = 0$).

When deriving QED from first principles, one often uses the minimal coupling Hamiltonian in the Coulomb gauge[44] [see Eq. (4)]. From there, the electric-dipole Hamiltonian can be found via a gauge transformation. The commonly used Pauli-Fierz (PF) QED Hamiltonian[17,21,47] [see Eq. (10)] in recent studies of polariton chemistry can be obtained by applying another gauge transformation on the electric-dipole Hamiltonian. We will further discuss the consequence of matter state truncation on gauge invariance, the connection with the commonly used quantum optics model Hamiltonians, and when they will break down in molecular QED.

When fixing a specific gauge, one defines the gauge-dependent vector and scalar potentials for the electromagnetic field. By choosing the Coulomb Gauge (i.e., by enforcing $\nabla\cdot\boldsymbol{A} = 0$) which makes the vector potential purely transverse, $\hat{\boldsymbol{A}} = \hat{\boldsymbol{A}}_\perp$, the Hamiltonian of point charge particles (including both electrons and nuclei) interacting with the electromagnetic field can be written as follows:[42]

$$\hat{H} = \sum_j^N \frac{1}{2m_j}(\hat{\mathbf{p}}_j - q_j\hat{\boldsymbol{A}}_\perp(\mathbf{r}_j))^2 + \frac{\epsilon_0}{2}\int dr^3\hat{\mathbf{E}}_\parallel^2(\mathbf{r}) + \frac{\epsilon_0}{2}\int dr^3\left[\hat{\mathbf{E}}_\perp^2(\mathbf{r}) + c^2\hat{\mathbf{B}}_\perp^2(\mathbf{r})\right], \tag{B1}$$

where the sum includes *both* the nuclear and electronic DOFs, $\mathbf{r}_j$ and $\mathbf{p}_j$ are the position and momentum of the charged particle j, with the charge q_j and mass m_j. Further, $\boldsymbol{A}_\perp(\mathbf{r})$, $\mathbf{E}_\perp(\mathbf{r})$, and $\mathbf{B}_\perp(\mathbf{r})$ are the transverse vector potential, electric field, and magnetic field, respectively. The energy associated with $\mathbf{E}_\parallel(\mathbf{r})$ [the second term in Eq. (B1)] is given by

$$\begin{aligned}\frac{\epsilon_0}{2}\int dr^3\hat{\mathbf{E}}_\parallel^2(\mathbf{r}) &= \sum_j \frac{q_j^2}{2\epsilon_0(2\pi)^3}\int\frac{dk^3}{k^2} + \frac{1}{8\pi\epsilon_0}\sum_{i\neq j}\frac{q_iq_j}{|\hat{\mathbf{x}}_i - \hat{\mathbf{x}}_j|}\\ &= \sum_j \epsilon_j^\infty + \hat{V}(\hat{\mathbf{x}}) \to \hat{V}(\hat{\mathbf{x}}).\end{aligned} \tag{B2}$$

Here, the first term $\sum_j\epsilon_j^\infty$ in the third line of Eq. (B2) is a time-independent infinite quantity that is referred to as the self-energy (not to be confused with the dipole self-energy), which can be regarded as a shift of the zero-point energy[157] and is dropped in the last line of the above equation. In short, the Coulomb potential $V_{\rm coul}(\hat{\mathbf{x}}) \equiv V(\hat{\mathbf{x}})$ emerges from the longitudinal electric field.

The last term in Eq. (B1) is the energy associated with the transverse fields $\hat{\mathbf{E}}_\perp(\mathbf{r})$ and $\hat{\mathbf{B}}_\perp(\mathbf{r})$. The general expressions for $\hat{\boldsymbol{A}}_\perp(\mathbf{r})$, $\hat{\mathbf{E}}_\perp(\mathbf{r})$, and $\hat{\mathbf{B}}_\perp(\mathbf{r})$ are[42]

$$\hat{\boldsymbol{A}}_\perp(\mathbf{r}) = \sum_{\mathbf{k}}\frac{\hat{\mathbf{e}}_{\mathbf{k}}}{\omega_{\mathbf{k}}}\sqrt{\frac{\hbar\omega_{\mathbf{k}}}{2\varepsilon_0\mathcal{V}}}(\hat{a}_{\mathbf{k}}e^{i\mathbf{k}\cdot\mathbf{r}} + \hat{a}_{\mathbf{k}}^\dagger e^{-i\mathbf{k}\cdot\mathbf{r}}), \tag{B3a}$$

$$\hat{\mathbf{E}}_\perp(\mathbf{r}) = i\sum_{\mathbf{k}}\hat{\mathbf{e}}_{\mathbf{k}}\sqrt{\frac{\hbar\omega_{\mathbf{k}}}{2\varepsilon_0\mathcal{V}}}(\hat{a}_{\mathbf{k}}e^{i\mathbf{k}\cdot\mathbf{r}} - \hat{a}_{\mathbf{k}}^\dagger e^{-i\mathbf{k}\cdot\mathbf{r}}), \tag{B3b}$$

$$\hat{\mathbf{B}}_\perp(\mathbf{r}) = i\sum_{\mathbf{k}}\frac{\mathbf{k}\times\hat{\mathbf{e}}_{\mathbf{k}}}{\omega_{\mathbf{k}}}\sqrt{\frac{\hbar\omega_{\mathbf{k}}}{2\varepsilon_0\mathcal{V}}}(\hat{a}_{\mathbf{k}}e^{i\mathbf{k}\cdot\mathbf{r}} - \hat{a}_{\mathbf{k}}^\dagger e^{-i\mathbf{k}\cdot\mathbf{r}}), \tag{B3c}$$

where $\hat{a}_{\mathbf{k}}^\dagger$ and $\hat{a}_{\mathbf{k}}$ are the raising and lowering operators of the mode that has a wavevector of $\mathbf{k} \equiv (k_x, k_y, k_z)$, and they satisfy the canonical commutation relation[42]

$$[\hat{a}_{\mathbf{k}}^\dagger, \hat{a}_{\mathbf{k}'}] = \delta_{\mathbf{k},\mathbf{k}'}\cdot\hat{\mathbb{1}}_{\mathbf{k}}. \tag{B4}$$

$\hat{a}_{\mathbf{k}}^\dagger$ and $\hat{a}_{\mathbf{k}}$ are the creation and annihilation operators of the photon, respectively, $\delta_{\mathbf{k},\mathbf{k}'}$ is the Kronecker delta, and the frequency of mode $\mathbf{k}$ is $\omega_j = c|\mathbf{k}|$. Here $\mathbf{k} = |\mathbf{k}|\hat{\mathbf{k}}$ aligns in the direction of the unit

13 February 2025 02:07:04

Published under an exclusive license by AIP Publishing

vector $\hat{\mathbf{k}}$ and $\hat{\mathbf{e}}_{\mathbf{k}} \perp \hat{\mathbf{k}}$ is the polarization unit vector for $\hat{\mathbf{E}}_\perp(\mathbf{r})$ and $\hat{\mathbf{A}}_\perp(\mathbf{r})$. The polarization of the photonic field can be written as a linear combination of the transverse electric (TE) polarization, $\hat{\mathbf{e}}_{\mathbf{k},\mathrm{TE}}$, and the transverse magnetic [TM] polarization, $\hat{\mathbf{e}}_{\mathbf{k},\mathrm{TM}}$, in relation to a given interface and propagation direction. The TE mode's polarization, $\hat{\mathbf{e}}_{\mathbf{k},\mathrm{TE}}$, is defined as being perpendicular to the propagation direction and parallel to the interface. The TM mode's polarization, $\hat{\mathbf{e}}_{\mathbf{k},\mathrm{TM}}$, is defined as being perpendicular to both the propagation direction and the TE polarization. For a given polarization, $\hat{\mathbf{e}}_{\mathbf{k}}$, the transverse electric field is along $\hat{\mathbf{e}}_{\mathbf{k}}$ and the magnetic field is along the $\hat{\mathbf{k}} \times \hat{\mathbf{e}}_{\mathbf{k}}$ direction. For example, for the TM mode, the transverse electric field polarization is along $\hat{\mathbf{e}}_{\mathbf{k},\mathrm{TE}}$ and the transverse magnetic field polarization is along $-\hat{\mathbf{e}}_{\mathbf{k},\mathrm{TM}}$.

When considering a planar Fabry–Pérot (FP) microcavity, $\hat{\mathbf{A}}_\perp(\mathbf{r})$, $\hat{\mathbf{E}}_\perp(\mathbf{r})$, and $\hat{\mathbf{B}}_\perp(\mathbf{r})$ satisfy the boundary conditions and thus the wavevector $\mathbf{k}$ becomes quantized.[42,157] For cavity mirrors imposing a boundary condition along z direction (see Fig. 8), the z component of the wavevector $k_z = n\frac{\pi}{L_z}$ with $n = 1, 2, 3\ldots$ as a positive integer. Note that k_x and k_y still remain quasi-continuous variables. These are discussed in detail in Sect. VI.

Using the above expressions, the energy of the transverse fields, i.e., the last term in Eq. (B1) is quantized as follows:

$$\frac{\varepsilon_0}{2}\int_{\mathcal{V}} dr^3 \left[\mathbf{E}_\perp^2(\mathbf{r}) + c^2\mathbf{B}_\perp^2(\mathbf{r})\right] = \sum_{\mathbf{k}}\left(\hat{a}_{\mathbf{k}}^\dagger \hat{a}_{\mathbf{k}} + \frac{1}{2}\right)\hbar\omega_{\mathbf{k}}, \tag{B5}$$

where the spatial integral dr^3 is done within the effective quantized volume $\mathcal{V}$ of the cavity. Thus, Eq. (B1) is quantized as

$$\hat{H}_{\mathrm{p}\cdot\mathrm{A}} = \sum_j^N \frac{1}{2m_j}(\hat{\mathbf{p}}_j - z_j\hat{\mathbf{A}}_\perp(\hat{\mathbf{x}}_j))^2 + \hat{V}(\hat{\mathbf{x}}) + \sum_{\mathbf{k}}\left(\hat{a}_{\mathbf{k}}^\dagger \hat{a}_{\mathbf{k}} + \frac{1}{2}\right)\hbar\omega_{\mathbf{k}}. \tag{B6}$$

This is commonly referred to as the "p · A" or the minimal coupling QED Hamiltonian, in the sense that the light and matter coupling is only carried through the matter momentum and the vector potential of the field. The minimal coupling structure in Eq. (4) comes naturally due to the local $U(1)$ symmetry of the EM field, which is an Abelian gauge field.

Assuming that the size of the molecular system is much smaller than the length of the cavity in the quantized direction, which is commonly referred to as the *long-wavelength approximation*, the transverse fields can be treated as spatially uniform, i.e., $e^{i\mathbf{k}\cdot\mathbf{r}} \approx 1$, such that

$$\hat{\mathbf{A}}_\perp(\mathbf{r}) \approx \hat{\mathbf{A}}_\perp = \sum_{\mathbf{k}} \frac{\hat{\mathbf{e}}_{\mathbf{k}}}{\omega_{\mathbf{k}}}\sqrt{\frac{\hbar\omega_{\mathbf{k}}}{2\varepsilon_0\mathcal{V}}}(\hat{a}_{\mathbf{k}} + \hat{a}_{\mathbf{k}}^\dagger). \tag{B7}$$

APPENDIX C: DERIVATION OF BAKER–CAMPBELL–HAUSDORFF IDENTITY

For the properly truncated Coulomb gauge Hamiltonian (see Sec. III C), the residual momentum, $\tilde{\mathbf{P}}_\mathbf{j}$, and the transformed electronic Hamiltonian, $\hat{\mathcal{U}}^\dagger\hat{\mathcal{H}}_{\mathrm{el}}\hat{\mathcal{U}}$, must be found by using the Baker–Campbell–Hausdorff (BCH) Identity, which is of the form

$$e^{\hat{A}}\hat{B}e^{-\hat{A}} = \hat{B} + [\hat{A},\hat{B}] + \frac{1}{2!}[\hat{A},[\hat{A},\hat{B}]] + \frac{1}{3!}[\hat{A},[\hat{A},[\hat{A},\hat{B}]]] + \cdots, \tag{C1}$$

where $\hat{A}$ and $\hat{B}$ are arbitrary operators.

To derive this identity, we first define a function $\hat{f}(\lambda)$,

$$\hat{f}(\lambda) = e^{\lambda\hat{A}}\hat{B}e^{-\lambda\hat{A}}, \tag{C2}$$

where λ is a scalar parameter. With this formalism, $\hat{f}(0) = \hat{B}$ and $\hat{f}(1) = e^{\hat{A}}\hat{B}e^{-\hat{A}}$. We can then write $f(1)$ by Taylor expanding about $\lambda = 0$,

$$\hat{f}(1) = \hat{B} + \sum_{n=1}^{\infty}\frac{1}{n!}\frac{\mathrm{d}\hat{f}^n(\lambda)}{\mathrm{d}\lambda^n}\Big|_{\lambda=0}\cdot(1-0)^n. \tag{C3}$$

By using the commutation relation, $[\hat{A}, \exp(\pm\lambda\hat{A})] = 0$, the first derivative of $\hat{f}(\lambda)$ can be expressed as

$$\begin{aligned}\frac{\mathrm{d}\hat{f}(\lambda)}{\mathrm{d}\lambda} &= e^{\lambda\hat{A}}\hat{A}\hat{B}e^{-\lambda\hat{A}} + e^{\lambda\hat{A}}\hat{B}(-\hat{A})e^{-\lambda\hat{A}} \\ &= e^{\lambda\hat{A}}[\hat{A},\hat{B}]e^{-\lambda\hat{A}}.\end{aligned} \tag{C4}$$

Similarly,

$$\begin{aligned}\frac{d^2\hat{f}(\lambda)}{d\lambda^2} &= e^{\lambda\hat{A}}(\hat{A}[\hat{A},\hat{B}] - [\hat{A},\hat{B}]\hat{A})e^{-\lambda\hat{A}} \\ &= e^{\lambda\hat{A}}[\hat{A},[\hat{A},\hat{B}]]e^{-\lambda\hat{A}}.\end{aligned} \tag{C5}$$

By recursion the nth derivative becomes apparent. Since the $\hat{B}$ in Eq. (C2) is any arbitrary operator, the nth derivative can be expressed in a similar manner to the first derivative

$$\frac{\mathrm{d}\hat{f}^n(\lambda)}{\mathrm{d}\lambda^n} = \left[\hat{A}, \frac{\mathrm{d}\hat{f}^{n-1}(0)}{\mathrm{d}\lambda^{n-1}}\right], \tag{C6}$$

where $d^{n-1}\hat{f}(0)/d\lambda^{n-1}$ is evaluated at $\lambda = 0$ so the $e^{\lambda\hat{A}} = e^{-\lambda\hat{A}} = \hat{\mathbb{1}}$. By evaluating Eq. (C6) at $\lambda = 0$ for each n and inputting the values into Eq. (C3), we get

$$\hat{f}(1) = \hat{B} + [\hat{A},\hat{B}] + \frac{1}{2!}[\hat{A},[\hat{A},\hat{B}]] + \frac{1}{3!}[\hat{A},[\hat{A},[\hat{A},\hat{B}]]] + \cdots, \tag{C7}$$

which perfectly agrees with the statement of the BCH identity in Eq. (C1).

REFERENCES

[1] J. A. Hutchison, T. Schwartz, C. Genet, E. Devaux, and T. W. Ebbesen, Angew. Chem. Int. Ed. **51**, 1592 (2012).
[2] A. Thomas, J. George, A. Shalabney, M. Dryzhakov, S. J. Varma, J. Moran, T. Chervy, X. Zhong, E. Devaux, C. Genet, J. A. Hutchison, and T. W. Ebbesen, Angew. Chem. Int. Ed. **55**, 11462 (2016).
[3] T. W. Ebbesen, Acc. Chem. Res. **49**, 2403 (2016).
[4] A. Thomas, L. Lethuillier-Karl, K. Nagarajan, R. M. A. Vergauwe, J. George, T. Chervy, A. Shalabney, E. Devaux, C. Genet, J. Moran, and T. W. Ebbesen, Science **363**, 615 (2019).
[5] A. Thomas, A. Jayachandran, L. Lethuillier-Karl, R. M. A. Vergauwe, K. Nagarajan, E. Devaux, C. Genet, J. Moran, and T. W. Ebbesen, Nanophotonics **9**, 249 (2020).
[6] A. Sau, K. Nagarajan, B. Patrahau, L. Lethuillier-Karl, R. M. A. Vergauwe, A. Thomas, J. Moran, C. Genet, and T. W. Ebbesen, Angew. Chem. Int. Ed. **60**, 5712 (2021).

13 February 2025 02:07:04

Published under an exclusive license by AIP Publishing

[7]J. Lather, P. Bhatt, A. Thomas, T. W. Ebbesen, and J. George, Angew. Chem. Int. Ed. **58**, 10635 (2019).
[8]J. Lather and J. George, J. Phys. Chem. Lett. **12**, 379 (2021).
[9]J. George, T. Chervy, A. Shalabney, E. Devaux, H. Hiura, C. Genet, and T. W. Ebbesen, Phys. Rev. Lett. **117**, 153601 (2016).
[10]R. M. A. Vergauwe, A. Thomas, K. Nagarajan, A. Shalabney, J. George, T. Chervy, M. Seidel, E. Devaux, V. Torbeev, and T. W. Ebbesen, Angew. Chem. Int. Ed. **58**, 15324 (2019).
[11]K. Hirai, J. A. Hutchison, and H. Uji-i, ChemPlusChem **85**, 1981 (2020).
[12]F. J. Garcia-Vidal, C. Ciuti, and T. W. Ebbesen, Science **373**, eabd0336 (2021).
[13]F. Herrera and F. C. Spano, Phys. Rev. Lett. **116**, 238301 (2016).
[14]M. Kowalewski, K. Bennett, and S. Mukamel, J. Chem. Phys. **144**, 054309 (2016).
[15]A. Semenov and A. Nitzan, J. Chem. Phys. **150**, 174122 (2019).
[16]J. Galego, C. Climent, F. J. Garcia-Vidal, and J. Feist, Phys. Rev. X **9**, 021057 (2019).
[17]V. Rokaj, D. M. Welakuh, M. Ruggenthaler, and A. Rubio, J. Phys. B: At. Mol. Opt. Phys. **51**, 034005 (2018).
[18]A. Mandal, S. M. Vega, and P. Huo, J. Phys. Chem. Lett. **11**, 9215 (2020).
[19]A. Mandal, T. D. Krauss, and P. Huo, J. Phys. Chem. B **124**, 6321 (2020).
[20]C. Schäfer, M. Ruggenthaler, V. Rokaj, and A. Rubio, ACS Photonics **7**, 975 (2020).
[21]C. Schäfer, M. Ruggenthaler, and A. Rubio, Phys. Rev. A **98**, 043801 (2018).
[22]M. Ruggenthaler, J. Flick, C. Pellegrini, H. Appel, I. V. Tokatly, and A. Rubio, Phys. Rev. A **90**, 012508 (2014).
[23]J. A. C. Gonzalez-Angulo and J. Yuen-Zhou, J. Chem. Phys. **152**, 161101 (2020).
[24]J. F. Triana, F. J. Hernández, and F. Herrera, J. Chem. Phys. **152**, 234111 (2020).
[25]P. Martinez, B. Rosenzweig, N. M. Hoffmann, L. Lacombe, and N. T. Maitra, J. Chem. Phys. **154**, 014102 (2021).
[26]K. B. Arnardottir, A. J. Moilanen, A. Strashko, P. Törmä, and J. Keeling, Phys. Rev. Lett. **125**, 233603 (2020).
[27]P. Forn-Díaz, L. Lamata, E. Rico, J. Kono, and E. Solano, Rev. Mod. Phys. **91**, 025005 (2019).
[28]A. F. Kockum, A. Miranowicz, S. D. Liberato, S. Savasta, and F. Nori, Nat. Rev. Phys. **1**, 19 (2019).
[29]A. L. Boité, Adv. Quantum Technol. **3**, 1900140 (2020).
[30]S. D. Liberato, Phys. Rev. Lett. **112**, 016401 (2014).
[31]O. D. Stefano, A. Settineri, V. Macrì, L. Garziano, R. Stassi, S. Savasta, and F. Nori, Nat. Phys. **15**, 803 (2019).
[32]D. D. Bernardis, T. Jaako, and P. Rabl, Phys. Rev. A **97**, 043820 (2018).
[33]D. D. Bernardis, P. Pilar, T. Jaako, S. D. Liberato, and P. Rabl, Phys. Rev. A **98**, 053819 (2018).
[34]L. A. Martínez-Martínez, R. F. Ribeiro, J. C. González-Angulo, and J. Yuen-Zhou, ACS Photonics **5**, 167 (2018).
[35]Y. Ashida, A. İmamoğlu, and E. Demler, Phys. Rev. Lett. **126**, 153603 (2021).
[36]M. A. D. Taylor, A. Mandal, W. Zhou, and P. Huo, Phys. Rev. Lett. **125**, 123602 (2020).
[37]A. Stokes and A. Nazir, Nat. Commun **10**, 499 (2019).
[38]F. J. Hernández and F. Herrera, J. Chem. Phys. **151**, 144116 (2019).
[39]B. M. Weight, T. D. Krauss, and P. Huo, J. Phys. Chem. Lett. **14**, 5901–5913 (2023). pMID.
[40]M. A. D. Taylor, B. M. Weight, and P. Huo, Phys. Rev. B **109**, 104305 (2024).
[41]E. A. Power and S. Zienau, Philos. Trans. R. Soc. A **251**, 427 (1959).
[42]C. Cohen-Tannoudji, J. Dupont-Roc, and G. Grynberg, *Photons and Atoms: Introduction to Quantum Electrodynamics* (Wiley, 1997).
[43]C. Gustin, S. Franke, and S. Hughes, arXiv:2208.11796 (2022).
[44]] D. P. Craig and T. Thirunamachandran, *Molecular Quantum Electrodynamics: An Introduction to Radiation-Molecule Interactions* (Dover Publications, 1998), p. 324.
[45]M. Göppert-Mayer, Ann. Phys. **18**, 466 (2009).
[46]J. Feist, A. I. Fernández-Domínguez, and F. J. García-Vidal, Nanophotonics **10**, 477 (2020).
[47]J. Flick, M. Ruggenthaler, H. Appel, and A. Rubio, Proc. Natl. Acad. Sci. **114**, 3026 (2017).
[48]J. Wang, B. Weight, and P. Huo, "Investigating Cavity Quantum Electrodynamics-Enabled Endo/Exo- Selectivities a diels-alder reaction," chemRxiv (2024).
[49]B. M. Weight, X. Li, and Y. Zhang, Phys. Chem. Chem. Phys. **25**, 31554 (2023).
[50]B. M. Weight, S. Tretiak, and Y. Zhang, Phys. Rev. A **109**, 032804 (2024).
[51]B. M. Weight, D. J. Weix, Z. J. Tonzetich, T. D. Krauss, and P. Huo, J. Am. Chem. Soc. **146**, 16184–16193 (2024).
[52]W. Ying and P. Huo, "Resonance theory of vibrational strong coupling enhanced polariton chemistry," chemRxiv (2024).
[53]W. Ying, M. A. D. Taylor, and P. Huo, Nanophotonics **13**, 2601 (2024).
[54]S. Montillo Vega, W. Ying, and P. Huo, "Theory of resonance suppression in vibrational polariton chemistry," chemRxiv (2024).
[55]N. M. Hoffmann, C. Schäfer, N. Säkkinen, A. Rubio, H. Appel, and A. Kelly, J. Chem. Phys. **151**, 244113 (2019).
[56]T. E. Li, H.-T. Chen, A. Nitzan, and J. E. Subotnik, Phys. Rev. A **101**, 033831 (2020).
[57]S. Shin and H. Metiu, J. Chem. Phys. **102**, 9285 (1995).
[58]A. Stokes and A. Nazir, "Gauge non-invariance due to material truncation in ultrastrong-coupling QED," arXiv:2005.06499 (2020).
[59]E. Rousseau and D. Felbacq, Sci. Rep **7**, 11115 (2017).
[60]A. Stokes and A. Nazir, Rev. Mod. Phys. **94**, 045003 (2022).
[61]M. Roth, F. Hassler, and D. P. DiVincenzo, Phys. Rev. Res. **1**, 033128 (2019).
[62]A. Settineri, O. D. Stefano, D. Zueco, S. Hughes, S. Savasta, and F. Nori, Phys. Rev. Res. **3**, 023079 (2021).
[63]W. E. Lamb, R. R. Schlicher, and M. O. Scully, Phys. Rev. A **36**, 2763 (1987).
[64]K. Rzazewski and R. W. Boyd, J. Mod. Optic. **51**, 1137 (2004).
[65]G. Barton, J. Phys. B: At. Mol. Phys. **7**, 2134 (1974).
[66]L. Garziano, A. Settineri, O. D. Stefano, S. Savasta, and F. Nori, Phys. Rev. A **102**, 023718 (2020).
[67]C. A. Mead and D. G. Truhlar, J. Chem. Phys. **77**, 6090 (1982).
[68]R. J. Cave and M. D. Newton, Chem. Phys. Lett. **249**, 15 (1996).
[69]H. Guo and D. R. Yarkony, Phys. Chem. Chem. Phys. **18**, 26335 (2016).
[70]T. Pacher, C. A. Mead, L. S. Cederbaum, and H. Köppel, J. Chem. Phys. **91**, 7057 (1989).
[71]J. E. Subotnik, E. C. Alguire, Q. Ou, B. R. Landry, and S. Fatehi, Acc. Chem. Res. **48**, 1340 (2015).
[72]G. A. Worth and L. S. Cederbaum, Annu. Rev. Phys. Chem. **55**, 127 (2004).
[73]R. J. Cave and M. D. Newton, J. Chem. Phys. **106**, 9213 (1997).
[74]E. K. Irish, J. Gea-Banacloche, I. Martin, and K. C. Schwab, Phys. Rev. B **72**, 195410 (2005).
[75]E. K. Irish, Phys. Rev. Lett. **99**, 173601 (2007).
[76]S. Schweber, Ann. Phys. (NY) **41**, 205 (1967).
[77]V. V. Albert, G. D. Scholes, and P. Brumer, Phys. Rev. A **84**, 042110 (2011).
[78]S. Agarwal, S. M. H. Rafsanjani, and J. H. Eberly, Phys. Rev. A **85**, 043815 (2012).
[79]B. Weight and P. Huo, "Ab initio approaches to simulate molecular polaritons: Properties and quantum dynamics," chemRxiv (2024).
[80]T. S. Haugland, E. Ronca, E. F. Kjønstad, A. Rubio, and H. Koch, Phys. Rev. X **10**, 041043 (2020).
[81]T. S. Haugland, C. Schäfer, E. Ronca, A. Rubio, and H. Koch, J. Chem. Phys. **154**, 094113 (2021).
[82]F. Pavošević, S. Hammes-Schiffer, A. Rubio, and J. Flick, J. Am. Chem. Soc. **144**, 4995 (2022).
[83]F. Pavošević and A. Rubio, J. Chem. Phys. **157**, 094101 (2022).
[84]J. McTague and J. J. Foley, J. Chem. Phys. **156**, 154103 (2022).
[85]A. E. DePrince, J. Chem. Phys. **154**, 094112 (2022).
[86]M. D. Liebenthal, N. Vu, and A. E. DePrince, J. Chem. Phys. **156**, 054105 (2022).
[87]J. Yang, Q. Ou, Z. Pei, H. Wang, B. Weng, Z. Shuai, K. Mullen, and Y. Shao, J. Chem. Phys. **155**, 064107 (2021).
[88]I. Mazin and Y. Zhang, arXiv:2411.15022 (2024).
[89]X. Li and Y. Zhang, arXiv:2310.18228 (2023).
[90]F. Pavošević, R. L. Smith, and A. Rubio, Nat. Commun. **14**, 2766 (2023).
[91]F. Pavošević, R. L. Smith, and A. Rubio, J. Phys. Chem. A **127**, 10184 (2023).
[92]J. J. Foley, J. F. McTague, and A. E. DePrince, Chem. Phys. Rev. **4**, 041301 (2023).
[93]R. Manderna, N. Vu, and J. J. Foley, J. Chem. Phys. **161**, 174105 (2024).
[94]P. Roden and J. J. Foley, J. Chem. Phys. **161**, 194103 (2024).
[95]N. Vu, D. Mejia-Rodriguez, N. P. Bauman, A. Panyala, E. Mutlu, N. Govind, and J. J. Foley, J. Chem. Theory Comput. **20**, 1214 (2024).
[96]N. Vu, G. M. McLeod, K. Hanson, and A. E. DePrince, J. Phys. Chem. A **126**, 9303 (2022).

13 February 2025 02:07:04

Published under an exclusive license by AIP Publishing

[97]M. D. Liebenthal, N. Vu, and A. E. DePrince, J. Phys. Chem. A **127**, 5264 (2023).
[98]M. D. Liebenthal and A. E. DePrince, J. Chem. Phys. **161**, 064109 (2024).
[99]J. D. Mallory and A. E. DePrince, Phys. Rev. A **106**, 053710 (2022).
[100]J. Yang, Z. Pei, E. C. Leon, C. Wickizer, B. Weng, Y. Mao, Q. Ou, and Y. Shao, J. Chem. Phys. **156**, 124104 (2022).
[101]X. Li, S. Tretiak, and Y. Zhang, arXiv:2410.16478 (2024).
[102]M. A. D. Taylor, A. Mandal, and P. Huo, Opt. Lett. **47**, 1446 (2022).
[103]E. T. Jaynes and F. W. Cummings, Proc. IEEE **51**, 89 (1963).
[104]B. Mischuck and K. Mølmer, Phys. Rev. A **87**, 022341 (2013).
[105]M. Hofheinz, E. M. Weig, M. Ansmann, R. C. Bialczak, E. Lucero, M. Neeley, A. D. O'Connell, H. Wang, J. M. Martinis, and A. N. Cleland, Nature **454**, 310 (2008).
[106]M. Hofheinz, H. Wang, M. Ansmann, R. C. Bialczak, E. Lucero, M. Neeley, A. D. O. Connell, D. Sank, J. Wenner, J. M. Martinis, and A. N. Cleland, Nature **459**, 546 (2009).
[107]H. Hübener, U. D. Giovannini, C. Schäfer, J. Andberger, M. Ruggenthaler, J. Faist, and A. Rubio, Nat. Mater. **20**, 438 (2021).
[108]M. Holthaus, J. Phys. B: At. Mol. Opt. Phys. **49**, 013001 (2016).
[109]H. Sambe, Phys. Rev. A **7**, 2203 (1973).
[110]D. J. Tannor, *Introduction to Quantum Mechanics: A Time-Dependent Perspective* (University Science Books, Mill Valley, 2007).
[111]J. H. Shirley, Phys. Rev. **138**, B979 (1965).
[112]A. Csehi, M. Kowalewski, G. J. Halász, and Á. Vibók, New J. Phys. **21**, 093040 (2019).
[113]L. Qiu, A. Mandal, O. Morshed, M. T. Meidenbauer, W. Girten, P. Huo, A. N. Vamivakas, and T. D. Krauss, J. Phys. Chem. Lett. **12**, 5030 (2021).
[114]T. E. Li, B. Cui, J. E. Subotnik, and A. Nitzan, Annu. Rev. Phys. Chem. **73**, 43–71 (2021).
[115]T. Schwartz, J. A. Hutchison, J. Léonard, C. Genet, S. Haacke, and T. W. Ebbesen, ChemPhysChem **14**, 125 (2013).
[116]A. Thomas, E. Devaux, K. Nagarajan, G. Rogez, M. Seidel, F. Richard, C. Genet, M. Drillon, and T. W. Ebbesen, Nano Lett. **21**, 4365 (2021).
[117]K. Nagarajan, A. Thomas, and T. W. Ebbesen, J. Am. Chem. Soc. **143**, 16877 (2021).
[118]K. Hirai, H. Ishikawa, T. Chervy, J. A. Hutchison, and H. Uji-i, Chem. Sci. **12**, 11986 (2021).
[119]K. Hirai and H. Uji-i, Chem. Lett. **50**, 727 (2021).
[120]S. Satapathy, M. Khatoniar, D. K. Parappuram, B. Liu, G. John, J. Feist, F. J. Garcia-Vidal, and V. M. Menon, Sci. Adv. **7**, eabj0997 (2021).
[121]W. M. Takele, F. Wackenhut, Q. Liu, L. Piatkowski, J. Waluk, and A. J. Meixner, J. Phys. Chem. C **125**, 14932 (2021).
[122]G. D. Wiesehan and W. Xiong, J. Chem. Phys. **155**, 241103 (2021).
[123]M. V. Imperatore, J. B. Asbury, and N. C. Giebink, J. Chem. Phys. **154**, 191103 (2021).
[124]J. Lather, A. N. K. Thabassum, J. Singh, and J. George, Chem. Sci. **13**, 195 (2022).
[125]R. H. Tichauer, J. Feist, and G. Groenhof, J. Chem. Phys. **154**, 104112 (2021).
[126]D. Sanvitto and S. Kéna-Cohen, Nat. Mater. **15**, 1061 (2016).
[127]A. Mandal, M. A. Taylor, B. M. Weight, E. R. Koessler, X. Li, and P. Huo, Chem. Rev. **123**, 9786 (2023).
[128]R. Pandya, A. Ashoka, K. Georgiou, J. Sung, R. Jayaprakash, S. Renken, L. Gai, Z. Shen, A. Rao, and A. J. Musser, Adv. Sci. **9**, 2105569 (2022).
[129]K. Georgiou, K. E. McGhee, R. Jayaprakash, and D. G. Lidzey, J. Chem. Phys. **154**, 124309 (2021).
[130]D. Xu, A. Mandal, J. M. Baxter, S.-W. Cheng, I. Lee, H. Su, S. Liu, D. R. Reichman, and M. Delor, arXiv:2205.01176 (2022).
[131]K. Georgiou, R. Jayaprakash, A. Othonos, and D. G. Lidzey, Angew. Chem. Int. Ed. **60**, 16661 (2021b).
[132]M. Balasubrahmaniyam, C. Genet, and T. Schwartz, Phys. Rev. B **103**, l241407 (2021).
[133]A. Graf, L. C. Tropf, Y. Zakharko, J. Zaumseil, and M. C. Gather, Nat. Commun. **7**, 13078 (2016).
[134]I. Vurgaftman, B. S. Simpkins, A. D. Dunkelberger, and J. C. Owrutsky, J. Phys. Chem. Lett. **11**, 3557 (2020).
[135]B. Xiang, R. F. Ribeiro, A. D. Dunkelberger, J. Wang, Y. Li, B. S. Simpkins, J. C. Owrutsky, J. Yuen-Zhou, and W. Xiong, Proc. Natl. Acad. Sci. **115**, 4845 (2018).
[136]T. Michalsky, H. Franke, R. Buschlinger, U. Peschel, M. Grundmann, and R. Schmidt-Grund, Eur. Phys. J. Appl. Phys. **74**, 30502 (2016).
[137]F. Hu and Z. Fei, Adv. Opt. Mater. **8**, 1901003 (2020).
[138]A. M. Berghuis, V. Serpenti, M. Ramezani, S. Wang, and J. G. Rivas, J. Phys. Chem. C **124**, 12030 (2020).
[139]A. M. Berghuis, R. H. Tichauer, L. M. A. de Jong, I. Sokolovskii, P. Bai, M. Ramezani, S. Murai, G. Groenhof, and J. G. Rivas, ACS Photonics **9**, 2263 (2022).
[140]J. Guan, J.-E. Park, S. Deng, M. J. H. Tan, J. Hu, and T. W. Odom, Chem. Rev. **122**, 15177 (2022).
[141]R. Guo, T. K. Hakala, and P. Törmä, Phys. Rev. B **95**, 155423 (2017).
[142]S. Baieva, O. Hakamaa, G. Groenhof, T. T. Heikkilä, and J. J. Toppari, ACS Photonics **4**, 28 (2017).
[143]C. Brimont, L. Doyennette, G. Kreyder, F. Réveret, P. Disseix, F. Médard, J. Leymarie, E. Cambril, S. Bouchoule, M. Gromovyi, B. Alloing, S. Rennesson, F. Semond, J. Zúñiga-Pérez, and T. Guillet, Phys. Rev. Appl. **14**, 054060 (2020).
[144]J. J. Hopfield, Phys. Rev. **112**, 1555 (1958).
[145]J. Keeling, *Light-Matter Interactions and Quantum Optics* (University of St. Andrews, 2012).
[146]J. Li, D. Golez, G. Mazza, A. J. Millis, A. Georges, and M. Eckstein, Phys. Rev. B **101**, 205140 (2020).
[147]M. Amin, E. R. Koessler, O. Morshed, F. Awan, N. M. Cogan, R. Collison, T. Tumiel, W. Girten, C. S. Leiter, A. N. Vamivakas, P. Huo, and T. D. Krauss, "Cavity controlled upconversion in CdSe nanoplatelet polaritons," chemRxiv (2024).
[148]F. Freire-Fernández, N. G. Sinai, M. J. Hui Tan, S.-M. Park, E. R. Koessler, T. Krauss, P. Huo, and T. W. Odom, ACS Nano **18**, 15177–15184 (2024).
[149]R. S. Mulliken, J. Am. Chem. Soc. **74**, 811 (1952).
[150]N. S. Hush, "Intervalence-transfer absorption. Part 2. Theoretical considerations and spectroscopic data," in *Progress in Inorganic Chemistry* (John Wiley & Sons, Ltd, 1967), pp. 391–444.
[151]T. J. Giese and D. M. York, J. Chem. Phys. **120**, 7939 (2004).
[152]T. V. Voorhis, T. Kowalczyk, B. Kaduk, L.-P. Wang, C.-L. Cheng, and Q. Wu, Annu. Rev. Phys. Chem. **61**, 149 (2010).
[153]J. E. Subotnik, S. Yeganeh, R. J. Cave, and M. A. Ratner, J. Chem. Phys. **129**, 244101 (2008).
[154]M. Kowalewski, K. Bennett, and S. Mukamel, J. Phys. Chem. Lett. **7**, 2050 (2016).
[155]A. Mandal and P. Huo, J. Phys. Chem. Lett. **10**, 5519 (2019).
[156]J. Fregoni, G. Granucci, E. Coccia, M. Persico, and S. Corni, Nat. Commun. **9**, 4688 (2018).
[157]G. Grynberg, A. Aspect, and C. Fabre, *Introduction to Quantum Optics from the Semi-Classical Approach to Quantized Light* (Cambridge University Press, 2010), p. 665.

13 February 2025 02:07:04

Published under an exclusive license by AIP Publishing